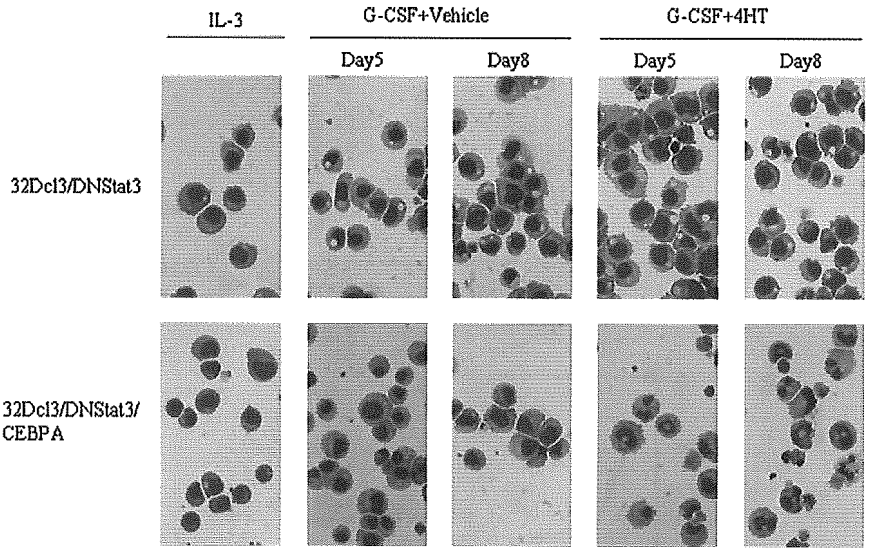

FIG. 6. **Morphologic features of 32Dcl3/DNStat3 and 32Dcl3/DNStat3/CEBPA cells.** Granulocytic differentiation of 32Dcl3/DNStat3 cells after induction of C/EBPα is shown. Cells were maintained in IL-3 and washed twice with PBS and then starved of cytokines for 8 h and stimulated with 10 ng/ml G-CSF plus 0.5 μM 4-HT or vehicle for 5 or 8 days. The cells were cytospun and stained with May-Grunwald and Giemsa stain (original magnification, ×400).

TABLE II
Differential count of 32Dcl3/DNStat3 and 32Dcl3/DNStat3/CEBPA cells

32Dcl3/DNStat3 and32Dcl3/DNStat3/CEBPA cells were maintained in IL-3 and starved of cytokines for 8 h and stimulated with 10 ng/ml G-CSF plus 0.5 μM 4-HT or vehicle for 5 days. Differential count was performed by May-Grunwald and Giemsa stain. Values are the mean ± S.D. percent of cells from three independent experiments. Myelocyte includes promyelocytes, myelocytes, and metamyelocytes. Band(seg) includes band and segmented neutrophils.

Cells	G-CSF+Vehicle	G-CSF+4HT
32Dcl3/DNStat3		
Myeloblasts	98.0 ± 0	99.3 ± 0.47
Myelocytes	1.3 ± 0.94	0.67 ± 0.47
Band(seg)	0.67 ± 0.94	0 ± 0
32Dcl3/DNStat3/CEBPA		
Myeloblasts	90.7 ± 3.3	3.0 ± 2.8
Myelocytes	5.0 ± 0.82	54.3 ± 2.4
Band(seg)	4.3 ± 2.6	42.7 ± 0.47

regulated C/EBPα function in the G-CSF signaling pathway, we transfected a C/EBPα-tamoxifen receptor fusion protein (C/EBPα-ER) into 32Dcl3 and 32Dcl3/DNStat3 cells (32Dcl3/CEBPA cells, 32Dcl3/DNStat3/CEBPA cells, respectively). The expression of C/EBPα-ER in these cells was verified by Western blotting (Fig. 5*A*). C/EBPα-ER localizes to the cytoplasm and is in an inactive form in the absence of tamoxifen. Upon treatment with tamoxifen, it translocates from cytoplasm to nucleus and becomes active. 32Dcl3, 32Dcl3/CEBPA, 32Dcl3/DNStat3, and 32Dcl3/DNStat3/CEBPA cells were cultured with G-CSF in the presence or absence of tamoxifen, and cell proliferation was examined by both counting viable cells and [^{3}H]thymidine incorporation. 32Dcl3/DNStat3 proliferated in response to G-CSF, and proliferation was not affected by the presence of tamoxifen. Conversely, G-CSF-induced proliferation of 32Dcl3/DNStat3/CEBPA cells in the presence of tamoxifen was dramatically reduced (Fig. 5, *B* and *C*).

32Dcl3/DNStat3 cells maintain morphologically immature characteristics and proliferate without granulocytic differentiation after G-CSF stimulation. We examined the morphological changes in 32Dcl3 and 32Dcl3/DNStat3 cells induced by G-CSF after translocation of C/EBPα from the cytoplasm to the nucleus. When tamoxifen was added to medium containing G-CSF, 32Dcl3/DNStat3/CEBPA cells rapidly began to differentiate into granulocytes, and 5 days later, about 40% of the cells were morphologically similar to mature neutrophils. In contrast, 32Dcl3/DNStat3/CEBPA cells cultured in G-CSF-containing medium without tamoxifen appeared immature with blast-like morphologic features (Fig. 6, Table II). To quantitatively analyze the difference in granulocyte maturation in 32Dcl3/DNStat3/CEBPA cells stimulated by G-CSF in the presence of tamoxifen, the mature granulocyte marker Gr-1 was monitored by FACS analysis. 32Dcl3 cells differentiate into Gr-1-positive neutrophils in response to G-CSF (Fig. 7*A*). As shown in Fig. 7*D*, Gr-1-positive cells were increased by the addition of tamoxifen in 32Dcl3/DNStat3/CEBPA cells treated with G-CSF, although low levels were detected in the absence of tamoxifen.

C/EBPα Up-regulates Genes That Are Related to Granulocytic Differentiation—In a conditional expression system, induction of C/EBPα leads to expression of granulocyte-specific genes, such as neutrophil primary granule genes (lysozyme M, *NGAL*) and the G-CSF receptor gene (17). In 32Dcl3/DNStat3 cells, the expression of these genes following G-CSF stimulation was inhibited (Fig. 8, *A*, *C*, and *E*). Interestingly, only *NGAL* was up-regulated by G-CSF in 32Dcl3/DNStat3/CEBPA cells following the restoration of C/EBPα (Fig. 8*B*). Conversely, the expression of lysozyme M and the G-CSF receptor were not changed by the restoration of C/EBPα (Fig. 8, *D* and *F*). These data suggest that regulatory factors in addition to C/EBPα may be involved in the induction of expression of granulocyte-specific genes by G-CSF.

DISCUSSION

G-CSF plays a pivotal role in granulopoiesis and granulocytic differentiation. The binding of G-CSF to its receptor leads to the activation of the Jak-Stat pathway, phosphatidylinositol-3 kinase pathway, and Ras-MAP kinase cascade (22). In the Jak-Stat pathway, G-CSF activates Jak1, Jak2, and Tyk2 followed by the activation of Stat1, Stat3, and Stat5 (7, 8).

Dominant-negative Stat3 inhibits G-CSF-induced transcriptional activity of Stat3 (Fig. 1*A*), as does G-CSF-induced granulocytic differentiation *in vitro* (11). Also, more transgenic mice with a targeted mutation of their G-CSF receptor that abolishes G-CSF-dependent Stat3 activation show severe neutropenia with an accumulation of immature myeloid precursors in their bone marrows (12). Consequently, Stat3 is thought to play an essential role in G-CSF-induced granulocytic differentiation.

32Dcl3 cells differentiate into neutrophils after treatment with G-CSF, and 32Dcl3/DNStat3 cells (32Dcl3 cells expressing dominant-negative Stat3) proliferate in G-CSF without differentiation. The degree of the phosphorylation of ERK1/2 by

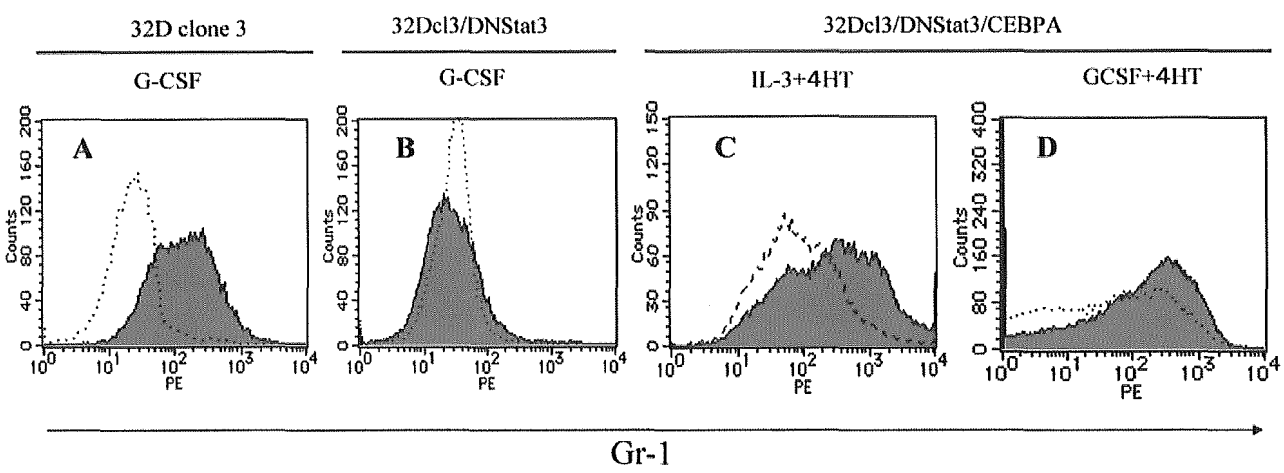

FIG. 7. **The expression of Gr-1 on 32Dcl3, 32Dcl3/DNStat3, and 32Dcl3/DNStat3/CEBPA cells.** 32Dcl3 (*A*) and 32Dcl3/DNStat3 cells (*B*) maintained in IL-3 (*broken line*) were starved of cytokines for 8 h and stimulated with 10 ng/ml G-CSF for 5 days (*solid line*). 32Dcl3/DNStat3/CEBPA (*C*) cells maintained in IL-3 were starved of cytokine for 8 h and stimulated with 1.0 ng/ml IL-3 (*C*) or 10 ng/ml G-CSF (*D*) plus 0.5 μM 4-HT (*solid line*) or vehicle (*broken line*) for 5 days.

G-CSF stimulation in 32Dcl3/DNStat3 cells was stronger than that in 32Dcl3 cells (Fig. 1*B*). We reported that Stat3 null bone marrow cells displayed a significant activation of ERK1/2 after G-CSF stimulation than wild-type bone marrow cells did using Stat3 conditional deficient mice (23). Then the augmented phosphorylation of ERK1/2 in response to G-CSF in 32Dcl3/DNStat3 cells might be caused by the functional abrogation of Stat3 in 32Dcl3/DNStat3 cells.

We compared gene profiles between two cell lines, 32Dcl3 and 32Dcl3/DNStat3 cells, to identify target genes of Stat3 in G-CSF signaling. We found that C/EBPα mRNA levels are rapidly up-regulated in 32Dcl3 cells following G-CSF treatment; these levels are increased 2.39-fold after 6 h and 4.20-fold after 48 h of treatment. In contrast to 32Dcl3 cells, C/EBPα mRNA levels are not changed in 32Dcl3/DNStat3 cells after G-CSF stimulation (Fig. 2*A*). The observation that cycloheximide does not inhibit G-CSF-induced increases in C/EBPα transcript levels (Fig. 2*B*) suggests that C/EBPα is induced by G-CSF directly downstream of Stat3. Dahl *et al.* (24) also reported that G-CSF induced the expression of C/EBPα in IL-3-dependent progenitors. *SOCS3* is one of the major target genes of Stat3. We previously reported that the expression level of SOCS3 protein in Stat3-deficient bone marrow cells is a trace, and it is not augmented by G-CSF stimulation (23). Contrary to this suppression of SOCS3 in Stat3-deficient cells, the induction of SOCS3 by G-CSF is not abolished in 32Dcl3/DNStat3 cells (data not shown).

The phosphorylation of ERK1/2 by G-CSF is stronger and the phosphorylation of Stat5 by IL-3 is weaker in 32Dcl3/DNStat3 cells when compared with those in 32D/Cl3 cells, although Stat1 phosphorylation by IFN-γ was not changed between these two cells (Figs. 1*B* and 3). Then there is the possibility that the transfection of dominant-negative Stat3 affects other signaling pathways in 32Dcl3/DNStat3 cells, resulting in the change of C/EBPα regulation. To clarify whether Stat3 directly up-regulates C/EBPα in the G-CSF signaling pathway in 32Dcl3 cells or not, we examined the effect of Stat3C on the transcription of C/EBPα. C/EBPα up-regulated the C/EBPα-dependent gene expression, and the G-CSF stimulation enhanced this C/EBPα-dependent gene expression (Fig. 4*A*). Strikingly, Stat3C augmented the C/EBPα-dependent gene expression as G-CSF stimulation did (Fig. 4, *B* and *C*). This means that G-CSF-induced up-regulation of C/EBPα-dependent gene expression is, at least partly, due to the activation of Stat3.

Two possibilities arise for the mechanism of the induction of C/EBPα transcription by activated Stat3 in the G-CSF signaling pathway. One is that activated Stat3 binds to the promoter region of *C/EBPα* and induces the transcription of C/EBPα. Analysis of the reported murine *C/EBPα* promoter sequence (20) identified no Stat-responsive elements (TTN5AA) (25, 26), but we found six Stat-responsive elements between 6 and 4 kb upstream of the *C/EBPα* transcription initiation site. Activated Stat3 might bind these Stat-responsive elements between 6 and 4 kb upstream of the C/EBPα transcription initiation site. The other possibility is that activated Stat3 might form the complex with C/EBPα and augment the transcriptional activity of C/EBPα because C/EBPα itself is the only protein reported to activate the murine *C/EBPα* promoter (20, 21). When a minimal TK promoter with CEBP-binding sites (p(C/EBP)2TK) together with C/EBPα was transfected to 293T cells, C/EBPα up-regulated C/EBPα-dependent gene expression. Activated Stat3 (Stat3C) enhanced this C/EBPα-dependent gene expression in collaboration with C/EBPα, although only Stat3C has no transcriptional activity on p(C/EBP)2TK (Fig. 4, *B* and *C*). In addition, the stimulation of G-CSF allows Stat3 to make the complex with C/EBPα (Fig. 4*D*). Then activated Stat3 by G-CSF makes the complex with C/EBPα and augments the transcriptional activity of C/EBPα. This is one of the reasons why induction of C/EBPα transcript through Stat3 activation by G-CSF occurred in 32Dcl3 cells. Several reports have described factors that repress *C/EBPα* promoter activity, such as SP1 (27), AP2A (28), or MYC (29). We show here for the first time that Stat3 augments the *C/EBPα* promoter activity.

Intracellular transcript levels of several genes were changed following G-CSF treatment downstream of Stat3 activation (Table I). To better identify the role of C/EBPα in Stat3-mediated signaling in G-CSF-induced granulocyte differentiation, C/EBPα-ER (C/EBPα-tamoxifen receptor fusion protein) was stably expressed in 32Dcl3 and 32Dcl3/DNStat3 cells. C/EBPα-ER translocates from the cytoplasm to the nucleus and becomes activated upon treatment with tamoxifen. Strikingly, transfection of C/EBPα-ER into 32Dcl3/DNStat3 cells abolished proliferation and induced myeloid differentiation by G-CSF without Stat3 activation (Figs. 5, *B* and *C*, and 6). These data indicate that C/EBPα activation induced by G-CSF through Stat3 plays an essential role in stopping the cell proliferation and inducing the differentiation to the myeloid lineage.

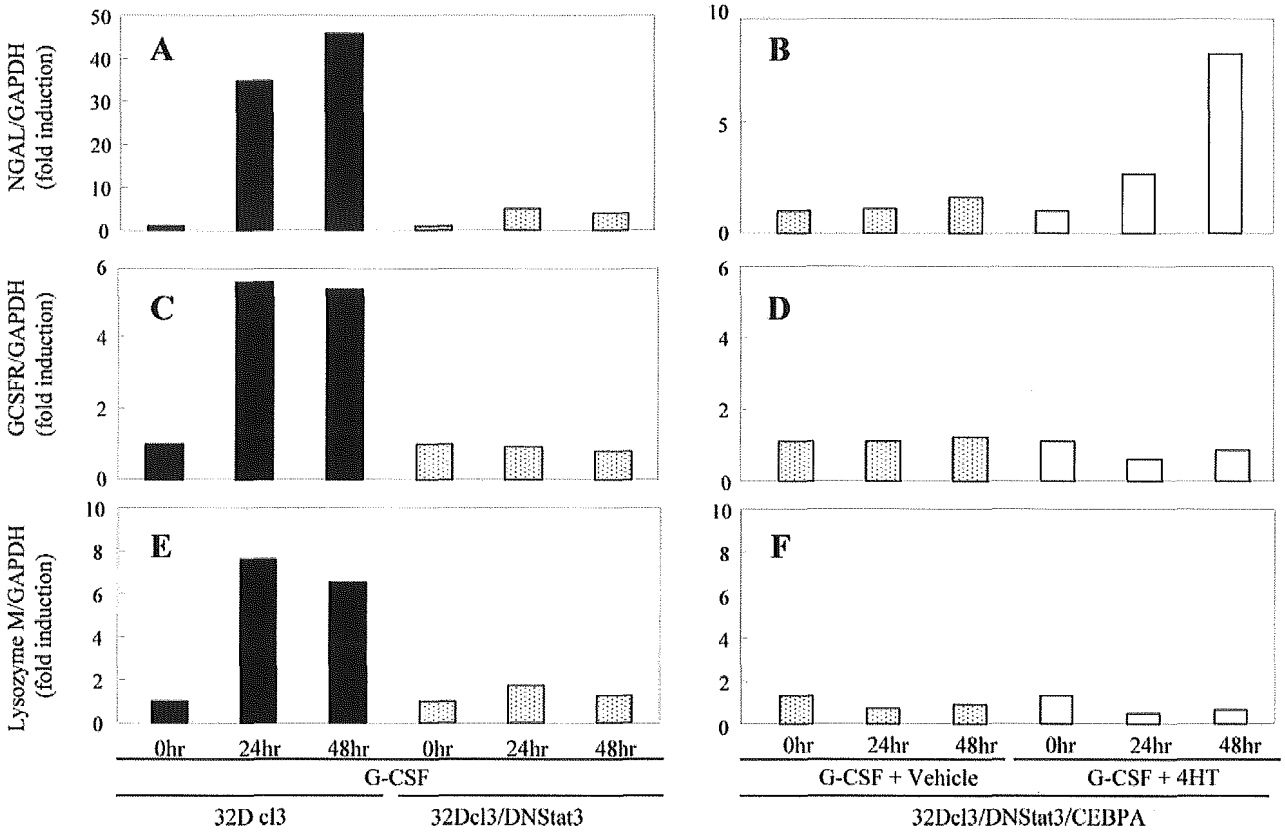

FIG. 8. **Granulocyte-specific gene expressions after C/EBPα induction.** The time course of NGAL (*A* and *B*), G-CSF receptor (*G-CSFR*) (*C* and *D*), and lysozyme M (*E* and *F*) mRNA expression following G-CSF stimulation in 32Dcl3 and 32Dcl3/DNStat3 cells (*A*, *C*, and *E*) or by G-CSF stimulation with 4-HT or vehicle in 32Dcl3/DNStat3/CEBPA cells (*B*, *D*, and *F*) is shown. Cells maintained in IL-3 were starved of cytokines for 8 h and stimulated with G-CSF, G-CSF, plus 4-HT and G-CSF plus vehicle. Total RNA was isolated at the indicated times after the stimulation and transcribed to cDNA, which was subjected to real-time PCR. The *numbers* given on the *vertical axis* represent the fold induction of ratios of average GAPDH-normalized expression values when compared with those before stimulation. Three independent experiments were performed, and similar results were obtained and shown data are the representative of them.

The CEBP family of transcription factor is expressed in multiple cell types, including hepatocytes, adipocytes, keratinocytes, enterocytes, and cells of the lung (30, 31). C/EBPα transactivates the promoters of hepatocyte- and adipocyte-specific genes, which are important for energy homeostasis (32, 33), and *C/EBPα*-deficient mice lack hepatic glycogen stores and die from hypoglycemia within 8 h of birth (34). In the hematopoietic system, C/EBPα is exclusively expressed in myelomonocytic cells (35, 36). C/EBPα expression is prominent in mature myeloid cells, and previous investigations found that C/EBPα is critical for early granulocytic differentiation. Mice with a targeted disruption of the *C/EBPα* gene demonstrate an early block in granulocytic differentiation, but they develop normal monocytes (19). Conditional expression of C/EBPα is sufficient to induce granulocytic differentiation (17). In contrast to the essential role of C/EBPα in granulocytic differentiation, the role of Stat in granulopoiesis is controversial. Stat3 is the principle Stat protein activated by G-CSF, with Stat5 and Stat1 also activated to a lesser degree (8, 10). In mice lacking *Stat5a* and *Stat5b*, the number of colonies produced in response to G-CSF was reduced 2-fold despite normal circulating numbers of neutrophils (9). Myeloid cell lines expressing dominant-negative forms of Stat3 (11, 37, 38) and transgenic mice with a targeted mutation of the G-CSF receptor that abolishes G-CSF-dependent Stat3 activation (12) demonstrate that Stat3-activation is required for G-CSF-dependent granulocytic proliferation and differentiation.

In the present study, we clearly demonstrate that the expression of C/EBPα mRNA is up-regulated through the activation of Stat3 in response to G-CSF, and the Stat3-C/EBPα signaling cascade plays an important role in G-CSF-induced differentiation. Contrary to these data, however, we and others showed that mice conditionally lacking Stat3 in their hematopoietic progenitors developed neutrophilia, and bone marrow cells were hyper-responsive to G-CSF stimulation (23, 39). Additionally, mice with tissue-specific disruption of *Stat3* in bone marrow cells die within 4–6 weeks after birth with Crohn's disease-like pathogenesis (40). These mice exhibit phenotypes with dramatic expansion of myeloid cells, leading to massive infiltration of the intestine with neutrophils, macrophages, and eosinophils. Cells of the myeloid lineage also demonstrate autonomous proliferation. These apparently disparate results may be explained by the need for molecules in addition to Stat3 to regulate C/EBPα expression *in vivo*, the *in vivo* functional redundancy among C/EBPα regulators, or the absence of the abrogation of SOCS3 induction by G-CSF in 32Dcl3/DNStat3 cells. In 32Dcl3 cells, the Stat3-C/EBPα pathway might be favored, and other pathways may contribute little to granulocytic differentiation in response to G-CSF.

Among C/EBP family, C/EBPε is important for late phase of granulocytic differentiation, and its expression is up-regulated by G-CSF independent of Stat3 (11). A previous report showed that C/EBPε is a transcriptional target of C/EBPα in 32Dcl3 cells (41). From these reports and our results, we speculated that a small amount of C/EBPα is enough for the induction of the transcription of C/EBPε by G-CSF or that there are multiple signaling steps except for Stat3-C/EBPα to induce the transcription of C/EBPε by G-CSF.

Induction of C/EBPα led to not only morphologic differentiation but also expression of granulocyte-specific genes (17). In 32Dcl3/DNStat3 cells, the induction of the G-CSF receptor, lysozyme M, and NGAL in response to G-CSF was abrogated (Fig. 8). Restoration of C/EBPα in these cells led to expression of only the *NGAL* gene, and thus, 32Dcl3/DNStat3 cells differentiated by the induction of C/EBPα may not be functional as mature neutrophils. In these cells, therefore, activation of C/EBPα is not sufficient for the induction of lysozyme M or G-CSF receptor genes, and the presence of other molecules appears to be required for their expression.

Acknowledgments—We thank M. Sato, R. Hasegawa, and M. Ito for excellent technical assistance.

REFERENCES

1. Metcalf, D. (1989) *Nature* **339,** 27–30
2. Demetri, G. D., and Griffin, J. D. (1991) *Blood* **78,** 2791–2808
3. Lieschke, G. J., Grail, D., Hodgson, G., Metcalf, D., Stanley, E., Cheers, C., Fowler, K. J., Basu, S., Zhan, Y. F., and Dunn, A. R. (1994) *Blood* **84,** 1737–1746
4. Liu, F., Wu, H. Y., Wesselschmidt, R., Kornaga, T., and Link, D. C. (1996) *Immunity* **5,** 491–501
5. Ihle, J. N., Nosaka, T., Thierfelder, W., Quelle, F. W., and Shimoda, K. (1997) *Stem Cells* **15,** Suppl. 1, 105–111; discussion 112
6. Ihle, J. N. (1995) *Nature* **377,** 591–594
7. Shimoda, K., Iwasaki, H., Okamura, S., Ohno, Y., Kubota, A., Arima, F., Otsuka, T., and Niho, Y. (1994) *Biochem. Biophys. Res. Commun.* **203,** 922–928
8. Shimoda, K., Feng, J., Murakami, H., Nagata, S., Watling, D., Rogers, N. C., Stark, G. R., Kerr, I. M., and Ihle, J. N. (1997) *Blood* **90,** 597–604
9. Teglund, S., McKay, C., Schuetz, E., van Deursen, J. M., Stravopodis, D., Wang, D., Brown, M., Bodner, S., Grosveld, G., and Ihle, J. N. (1998) *Cell* **93,** 841–850
10. Tian, S. S., Lamb, P., Seidel, H. M., Stein, R. B., and Rosen, J. (1994) *Blood* **84,** 1760–1764
11. Nakajima, H., and Ihle, J. N. (2001) *Blood* **98,** 897–905
12. McLemore, M. L., Grewal, S., Liu, F., Archambault, A., Poursine-Laurent, J., Haug, J., and Link, D. C. (2001) *Immunity* **14,** 193–204
13. Fukunaga, R., Ishizaka-Ikeda, E., Seto, Y., and Nagata, S. (1990) *Cell* **61,** 341–350
14. Reddy, V. A., Iwama, A., Iotzova, G., Schulz, M., Elsasser, A., Vangala, R. K., Tenen, D. G., Hiddemann, W., and Behre, G. (2002) *Blood* **100,** 483–490
15. Bromberg, J. F., Wrzeszczynska, M. H., Devgan, G., Zhao, Y., Pestell, R. G., Albanese, C., and Darnell, J. E., Jr. (1999) *Cell* **98,** 295–303
16. Aoki, N., and Matsuda, T. (2002) *Mol. Endocrinol.* **16,** 58–69
17. Radomska, H. S., Huettner, C. S., Zhang, P., Cheng, T., Scadden, D. T., and Tenen, D. G. (1998) *Mol. Cell. Biol.* **18,** 4301–4314
18. Wang, X., Scott, E., Sawyers, C. L., and Friedman, A. D. (1999) *Blood* **94,** 560–571
19. Zhang, D. E., Zhang, P., Wang, N. D., Hetherington, C. J., Darlington, G. J., and Tenen, D. G. (1997) *Proc. Natl. Acad. Sci. U. S. A.* **94,** 569–574
20. Christy, R. J., Kaestner, K. H., Geiman, D. E., and Lane, M. D. (1991) *Proc. Natl. Acad. Sci. U. S. A.* **88,** 2593–2597
21. Legraverend, C., Antonson, P., Flodby, P., and Xanthopoulos, K. G. (1993) *Nucleic Acids Res.* **21,** 1735–1742
22. Ihle, J. N. (1996) *BioEssays* **18,** 95–98
23. Kamezaki, K., Shimoda, K., Numata, A., Haro, T., Kakumitsu, H., Yosie, M., Yamamoto, M., Takeda, K., Matsuda, T., Akira, S., Ogawa, K., and Harada, M. (2005) *Stem Cells* **23,** 252–263
24. Dahl, R., Walsh, J. C., Lancki, D., Laslo, P., Iyer, S. R., Singh, H., and Simon, M. C. (2003) *Nat. Immunol.* **4,** 1029–1036
25. Horvath, C. M., Wen, Z., and Darnell, J. E., Jr. (1995) *Genes Dev.* **9,** 984–994
26. Xu, X., Sun, Y. L., and Hoey, T. (1996) *Science* **273,** 794–797
27. Tang, Q. Q., Jiang, M. S., and Lane, M. D. (1999) *Mol. Cell. Biol.* **19,** 4855–4865
28. Jiang, M. S., Tang, Q. Q., McLenithan, J., Geiman, D., Shillinglaw, W., Henzel, W. J., and Lane, M. D. (1998) *Proc. Natl. Acad. Sci. U. S. A.* **95,** 3467–3471
29. Mink, S., Mutschler, B., Weiskirchen, R., Bister, K., and Klempnauer, K. H. (1996) *Proc. Natl. Acad. Sci. U. S. A.* **93,** 6635–6640
30. Johnson, P. F., Landschulz, W. H., Graves, B. J., and McKnight, S. L. (1987) *Genes Dev.* **1,** 133–146
31. Landschulz, W. H., Johnson, P. F., Adashi, E. Y., Graves, B. J., and McKnight, S. L. (1988) *Genes Dev.* **2,** 786–800
32. Costa, R. H., Grayson, D. R., Xanthopoulos, K. G., and Darnell, J. E., Jr. (1988) *Proc. Natl. Acad. Sci. U. S. A.* **85,** 3840–3844
33. Lin, F. T., and Lane, M. D. (1994) *Proc. Natl. Acad. Sci. U. S. A.* **91,** 8757–8761
34. Wang, N. D., Finegold, M. J., Bradley, A., Ou, C. N., Abdelsayed, S. V., Wilde, M. D., Taylor, L. R., Wilson, D. R., and Darlington, G. J. (1995) *Science* **269,** 1108–1112
35. Scott, L. M., Civin, C. I., Rorth, P., and Friedman, A. D. (1992) *Blood* **80,** 1725–1735
36. Natsuka, S., Akira, S., Nishio, Y., Hashimoto, S., Sugita, T., Isshiki, H., and Kishimoto, T. (1992) *Blood* **79,** 460–466
37. Shimozaki, K., Nakajima, K., Hirano, T., and Nagata, S. (1997) *J. Biol. Chem.* **272,** 25184–25189
38. de Koning, J. P., Soede-Bobok, A. A., Ward, A. C., Schelen, A. M., Antonissen, C., van Leeuwen, D., Lowenberg, B., and Touw, I. P. (2000) *Oncogene* **19,** 3290–3298
39. Lee, C. K., Raz, R., Gimeno, R., Gertner, R., Wistinghausen, B., Takeshita, K., DePinho, R. A., and Levy, D. E. (2002) *Immunity* **17,** 63–72
40. Welte, T., Zhang, S. S., Wang, T., Zhang, Z., Hesslein, D. G., Yin, Z., Kano, A., Iwamoto, Y., Li, E., Craft, J. E., Bothwell, A. L., Fikrig, E., Koni, P. A., Flavell, R. A., and Fu, X. Y. (2003) *Proc. Natl. Acad. Sci. U. S. A.* **100,** 1879–1884
41. Wang, Q. F., and Friedman, A. D. (2002) *Blood* **99,** 2776–2785

ELSEVIER

International Journal of Cardiology 102 (2005) 233–238

International Journal of Cardiology

www.elsevier.com/locate/ijcard

Gene expression profiling of human atrial myocardium with atrial fibrillation by DNA microarray analysis

Ruri Ohki[a], Keiji Yamamoto[a,*], Shuichi Ueno[a], Hiroyuki Mano[b], Yoshio Misawa[c] Katsuo Fuse[c], Uichi Ikeda[a], Kazuyuki Shimada[a]

[a]*Division of Cardiovascular Medicine, Jichi Medical School, Minamikawachi-Machi, Tochigi 329-0498, Japan*
[b]*Division of Functional Genomics, Jichi Medical School, Minamikawachi-Machi, Tochigi 329-0498, Japan*
[c]*Division of Cardiovascular Surgery, Jichi Medical School, Minamikawachi-Machi, Tochigi 329-0498, Japan*

Received 16 December 2003; received in revised form 31 March 2004; accepted 5 May 2004
Available online 9 August 2004

Abstract

Background: Atrial fibrillation (AF) is the most frequently encountered arrhythmia in the clinical setting. However, a comprehensive investigation of the molecular mechanism of AF has not been performed. The aim of this study was to clarify transcriptional profiling of genes modulated in the atrium of AF patients using DNA microarray technology.
Methods: We obtained 17 fresh cardiac specimens, right atrial appendages, isolated from 10 patients with normal sinus rhythm and seven chronic AF patients who underwent cardiac surgery. Affymetrix GeneChip (Human Genome U95A) investigating 12,000 human genes was used for each specimen. Quantitative analysis of selected genes was performed by the real-time PCR method.
Results: The left atrial diameter in the AF group was greater than that in the sinus rhythm group. We could identify 33 AF-specific genes that were significantly activated (>1.5-fold), compared with the sinus rhythm group, including an ion channel, an antioxidant, an inflammation, three cell growth/cell cycle, three transcription such as nuclear factor-interleukin 6-beta, several cell signaling and several protein genes, and seven expressed sequence tags (ESTs). In contrast, we found 63 sinus rhythm-specific genes, including several cell signaling/communication such as sarcoplasmic reticulum Ca^{2+}-ATPase 2, several cellular respiration and energy production and two antiproliferative or negative regulator of cell growth genes, and 22 ESTs.
Conclusions: The present study demonstrated that about one hundred genes were modulated in the atria of AF patients. These findings suggest that these genes may play critical roles in the initiation or perpetuation of AF and the pathophysiology of atrial remodeling.

Keywords: Atrial fibrillation; Genes; Microarray; Myocardium

1. Introduction

Atrial fibrillation (AF) is the most common sustained cardiac arrhythmia and the major cardiac cause of stroke [1]. The Framingham Study [2] reported a sixfold increase in the incidence of stroke in patients with AF, compared with age-, sex-, and blood pressure-adjusted control subjects. In addition, the rapid heart rate resulting from AF can bring about a number of adverse outcomes including congestive heart failure and tachycardia-related cardiomyopathy [3,4]. The molecular research of AF has been focused mainly at various ion channels and at proteins involved in calcium homeostasis, because AF modifies the electrical properties of the atrium in a manner that promotes its occurrence and maintenance. This arrhythmogenic electrophysiological remodeling is well established. However, a comprehensive investigation of the molecular mechanism causing AF has not been performed.

With the recent discovery of the complete sequence of the human genome, as well as the genomes of other organisms, new high-throughput approaches to studying these complex pathways have been made possible. By

* Corresponding author. Tel.: +81 285 58 7344; fax: +81 285 44 5317.
E-mail address: kyamamoto@jichi.ac.jp (K. Yamamoto).

0167-5273/$ - see front matter © 2004 Elsevier Ireland Ltd. All rights reserved.
doi:10.1016/j.ijcard.2004.05.026

Table 1
Patient characteristics

Variable	Total (n=17)	AF (n=7)	Sinus rhythm (n=10)
Age (yrs)	59 ± 16	64 ± 9	56 ± 18
Left atrial diameter (mm)	52 ± 15	67 ± 9*	42 ± 7
LV ejection fraction (%)	60 ± 13	62 ± 13	58 ± 14
MR grade	2.2 ± 1.4	2.7 ± 1.0	1.8 ± 1.0
TR grade	2.0 ± 1.4	2.7 ± 1.0	1.5 ± 1.0
Systolic PA pressure (mmHg)	39.9 ± 14.0	45.0 ± 14.0	35.4 ± 14.0
Mean RA pressure (mmHg)	6.5 ± 3.5	8.6 ± 4.0	4.8 ± 1.0
Digitalis (n)	9	7	2
Systolic blood pressure (mmHg)	133 ± 25	134 ± 26	133 ± 25
Diastolic blood pressure (mmHg)	71 ± 16	75 ± 20	69 ± 13
Fasting blood sugar (mg/dl)	101 ± 15	90 ± 7†	107 ± 15
Total cholesterol (mg/dl)	195 ± 44	208 ± 41	189 ± 46
Triglyceride (mg/dl)	123 ± 64	118 ± 54	125 ± 71

Data are mean ±S.D. or n. *P<0.001 and †P<0.02 compared with sinus rhythm patients. AF, atrial fibrillation; LV, left ventricular; MR, mitral valve regurgitation; PA, pulmonary arterial; RA, right atrial; TR, tricuspid valve regurgitation.

using multiple cDNA or oligonucleotide samples placed on a glass slide, investigators can analyze several thousand full-length genes or expressed oligonucleotide sequences at once. In addition to identifying large clusters of genes that respond to a given stimulus, DNA microarray technology may be used to identify some genes that comprise highly specific molecular responses [5,6]. Already, some studies using microarray technology have yielded interesting results regarding the pathogenesis of cardiovascular diseases, such as myocardial infarction [7], cardiac hypertrophy [8], and human heart failure [9]. In the present study, we used DNA microarray technology to investigate the transcriptional profiling of genes modulated in the right atrium of patients with AF compared with sinus rhythm.

2. Methods

2.1. Subjects

This study group consisted of seven patients with AF (mean age 64±9 years) and 10 patients with sinus rhythm (mean age 56±18 years) who underwent cardiac surgery (Table 1). The underlying heart diseases in the patients are shown in Table 2. Hemodynamic studies were performed the morning after an overnight fast. Vasodilators were withheld for at least 24 h before evaluation. Chronic, stable doses of digoxin, and diuretics were continued but were administered on an evening schedule. Right and left heart studies, including measurement of pressure, biplane left ventriculography and coronary angiography, were performed using a percutaneous cathether. Left ventricular ejection fraction was determined by the area-length method [10]. The severity of mitral regurgitation was assessed according to the method of Sellers et al. [11]. Transthoracic echocardiography was performed in all patients using a Hewlett-Packard SONOS 5500 system (Hewlett-Packard, Palo Alto, CA) with a 2.5 MHz transducer. The left atrial diameter was determined by M-mode echocardiography [12]. The severity of tricuspid regurgitation was graded on a four-point scale, based on the distance reached by the abnormal signals from the tricuspid orifice toward the posterior wall in the parasternal four-chamber view [13].

This study was approved by our institutional human investigations committee, and written informed consent was obtained from all patients before participation.

2.2. Atrial myocardium samples

Right atrial appendages were obtained from the patients during cardiac surgery. Pieces of right atrial appendage weighing 200–1400 mg were frozen immediately in liquid nitrogen, and stored at −80 °C.

Table 2
Underlying heart disease

Patients	Age	Sex	Diagnosis
Sinus group			
1	44	M	AR
2	70	F	MR
3	75	M	AP
4	65	M	AS
5	60	M	AS
6	64	F	MR
7	64	F	AR, MR
8	15	M	ASD
9	63	M	AR
10	36	F	ASD
AF group			
1	51	F	MS
2	55	M	MR
3	64	M	MR
4	74	F	ASR, MSR
5	75	M	ASR, MR
6	59	F	MS
7	69	F	MSR

AP, angina pectoris; AR, aortic valve regurgitation; AS, aortic valve stenosis; ASD, atrial septal defect; ASR, aortic valve stenosis and regurgitation; MR, mitral valve regurgitation; MS, mitral valve stenosis; MSR, mitral valve stenosis and regurgitation.

2.3. Transcriptional profiling

A DNA microarray was used for each specimen. Total RNA was extracted using RNAzol B (TEL-TEST, Friendswood, TX), and the purity was checked by spectrophotometry and agarose gel electrophoresis. Total RNA (5 μg) was converted to double-stranded cDNA using an oligo dT primer containing the T7 promoter (Gibco BRL Superscript® Choice System; Life Technologies, Rockville, MD), and the template for an in vitro transcription reaction was used to synthesize biotin-labeled antisense cRNA (BioArray™ High Yield RNA Transcript Labeling Kit; Enzo Diagnostics, Farmingdale, NY). The biotinylated cRNA was fragmented and hybridized for 16 h at 45 °C to GeneChip Test2 arrays (Affymetrix, Santa Clara, CA) to assess sample quality, and then to Human Genome arrays (U95A, Affymetrix). The arrays were washed, and then stained with streptavidin-phycoerythrin. The arrays were scanned with the GeneArray scanner (Agilent Technologies, Palo Alto, CA) and analyzed using the GeneSpring software package (Silicon Genetics, Redwood City, CA). Human Genome U95A was derived from GenBank 113 and dbEST/10-02-99.

Detailed protocols for data analysis of Affymetrix oligonucleotide microarrays and extensive documentation of the sensitivity and quantitative aspects of the method have been described [14–16]. Briefly, each gene is represented by the use of ~20 perfectly matched (PM) and mismatched (MM) control probes. The MM probes act as specificity controls that allow the direct subtraction of both background and cross-hybridization signals. The number of instances in which the PM hybridization signal is larger than the MM signal is computed along with the average of the logarithm of the PM:MM ratio (after background subtraction) for each probe set. These values are used to make a matrix-based decision concerning the presence or absence of an RNA molecule. Positive average signal intensities after background subtraction were observed for over 12,000 genes for all samples. To determine the quantitative RNA abundance, the average of the differences representing PM minus MM for each gene-specific probe family is calculated, after discarding the maximum, the minimum, and any outliers beyond 3 SDs.

2.4. Real-time reverse transcription (RT)-PCR analysis

For reverse transcription (RT), RNA obtained from each specimen was reverse transcribed using T7-dT primer (5′-TCT AGT CGA CGG CCA GTG AAT TGT AAT ACG ACT CAC TAT AGG GCG TTT TTT TTT TTT TTT TTT TTT-3′) and Superscript II reverse transcriptase (Life Technologies). Real-time quantitative PCR was performed in optical tubes in a 96-well microtiter plate (Perkin-Elmer/Applied Biosystems, Foster City, CA) with an ABI PRISM 7700 Sequence Detector Systems (Perkin-Elmer/Applied Biosystems) according to the manufacturer's instructions. By using the SYBR Green PCR Core Reagents Kit (Perkin-Elmer/Applied Biosystems, P/N 4304886), fluorescence signals were generated during each PCR cycle via the 5′-to 3′-endonuclease activity of Taq Gold [17] to provide real-time quantitative PCR information. The oligonucleotide primers used for real-time PCR analysis are shown in Table 3. No template controls as well as the samples were added in a total volume of 50 μl/reaction. Potential PCR product contamination was digested by uracil-*N*-glycosylase, because dTTP is substituted by dUTP [17]. All PCR experiments were performed with the hot start method. In the reaction system, uracil-*N*-glycosylase and Taq Gold (Perkin-Elmer/Applied Biosystems) were applied according to the manufacturer's instructions [17,18]. Denaturing and annealing reactions were performed 40 times at 95 °C for 15 s, and at 60 °C for sarcoplasmic reticulum Ca^{2+}-ATPase 2, 66 °C for nuclear factor-interleukin 6 (NF-IL6)-beta and 62 °C for glyceraldehyde-3 phosphate dehydrogenase (GAPDH) for 1 min, respectively. The increase in the fluorescence signal is proportional to the amount of specific product [14]. The intensity of emission signals in each sample was normalized to that of GAPDH as an internal control.

2.5. Statistical analysis

Raw data from array scans were averaged across all gene probes for each array, and a scaling factor was applied to bring the average intensity for all probes on the array to 2500. This allows any sample to be normalized for comparison with any other comparable sample.

Table 3
Primer design for real-time PCR analysis

Gene		Primer sequence	PCR product size (bp)
NF-IL6-beta	Sense	5′-CACAGACCGTGGTGAGCTTG-3′	257
	Antisense	5′-CACCAACTTCTGCTGCATCTC-3′	
Sarcoplasmic reticulum	Sense	5′-TTTCTGGTACAAACATTGCTGC-3′	140
Ca^{2+}-ATPase 2	Antisense	5′-TAGTTTTTGCTGAAGGGGTGTT-3′	
GAPDH	Sense	5′-CTTTGGTATCGTGGAAGGACTC-3′	140
	Antisense	5′-CAGTAGAGGCAGGGATGATGTT-3′	

GAPDH, glyceraldehyde-3 phosphate dehydrogenase; NF-IL6, nuclear factor-interleukin 6.

Table 4
Analysis of AF-specific genes by DNA microarray

Function	Gene	Fold change	Genbank#
Antioxidants	Glutathione peroxidase	1.8 ± 1.1	X13710
Cell growth	Vascular endothelial growth factor B	1.6 ± 0.7	U43368
Cell signaling	RhoC	1.6 ± 0.5	L25081
Inflammation	Macrophage migration inhibitory factor	1.7 ± 0.6	L19686
Proto-oncogene	A-raf-1 oncogene	1.5 ± 0.5	U01337
Transcription	NF-IL6-beta	2.0 ± 0.7	M83667

Data are mean ±S.D. Fold change was relative to sinus rhythm group. NF-IL6, nuclear factor-interleukin 6.

Data are expressed as the mean ± S.D. Differences were analyzed with the Mann–Whitney *U* test for unpaired observations. A *P*-value of <0.05 was considered significant.

3. Results

3.1. Patient characteristics

As shown in Table 1, the left atrial diameter in the AF group was significantly greater than that in the sinus rhythm group ($P<0.001$). In addition, the levels of fasting blood sugar in the AF group were significantly lower than those in the sinus rhythm group ($P<0.02$). There were no other differences detected between the sinus rhythm group and AF group.

3.2. DNA microarray analysis of AF-specific genes

We identified 33 AF-specific genes that were significantly activated (>1.5-fold, $P<0.05$), compared with those in the sinus rhythm group, including an ion channel, an antioxidant, an inflammation, three cell growth/cell cycle, three transcription, several cell signaling and several protein genes, and seven expressed sequence tags (ESTs). Some of the selected genes are shown in Table 4. All data are available in an online only Data Supplement at http://www.elsevier.com/locate/inca/506041.

3.3. DNA microarray analysis of sinus rhythm-specific genes

In contrast, we found 63 sinus rhythm-specific genes, including several cell signaling/communication genes such as sarcoplasmic reticulum Ca^{2+}-ATPase 2, several cellular respiration and energy production and two antiproliferative or negative regulator of cell growth genes, and 22 ESTs (<0.5-fold, $P<0.05$). Some of the selected genes are shown in Table 5. All data are available in an online only Data Supplement at http://www.elsevier.com/locate/inca/506041.

3.4. Real-time RT-PCR analysis

We focused on two of the genes screened by the oligonucleotide microarray: NF-IL6-beta and sarcoplasmic reticulum Ca^{2+}-ATPase 2. NF-IL6-beta is an important transcriptional activator in the regulation of genes involved in the immune and inflammatory response [19]. AF may persist due to structural changes in the atria that are promoted by inflammation [20]. In addition, cytosolic Ca^{2+} overload may be an important mediator of AF. Abnormalities in the Ca^{2+} regulatory proteins, such as sarcoplasmic reticulum Ca^{2+}-ATPase 2, of the atrial myocardium in chronic AF patients may be involved in the initiation and/or perpetuation of AF. These genes were confirmed by the real-time RT-PCR method. As shown in Fig. 1, NF-IL6-beta mRNA expression in the AF group was significantly higher than that in the sinus rhythm group ($P<0.02$). In contrast, as shown in Fig. 2, sarcoplasmic reticulum Ca^{2+}-ATPase 2 mRNA expression in the AF group was lower compared with that in the sinus rhythm group ($P<0.1$), but not significantly.

4. Discussion

The cellular and molecular basis of AF has been a field of enormous interest over the past few years. However, the

Table 5
Analysis of sinus rhythm-specific genes by DNA microarray

Function	Gene	Fold change	Genbank#
Antioxidants	Peroxiredoxin 3	0.5 ± 0.2	D49396
Cell signaling	Caveolin 2	0.4 ± 0.3	AF035752
Cell signaling	Sarcoplasmic reticulum Ca^{2+}-ATPase 2	0.4 ± 0.3	M23115
Cell signaling	Connexin 43	0.4 ± 0.3	X52947
Proto-oncogene	Ras-associated protein rab1	0.5 ± 0.2	AL050268

Data are mean ±S.D. Fold change was relative to sinus rhythm group.

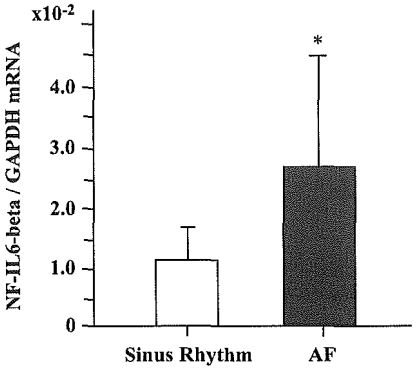

Fig. 1. Nuclear factor-interleukin 6 (NF-IL6)-beta mRNA expression in the right atria of patients with sinus rhythm and atrial fibrillation (AF). Total RNA obtained from the right atria of patients with sinus rhythm (n=10) and AF (n=7) using RNAzol B (TEL-TEST) was analyzed by quantitative real-time reverse transcription-PCR as described in Methods. The amount of mRNA expression for NF-IL6-beta was standardized to that of glyceraldehyde-3 phosphate dehydrogenase (GAPDH) mRNA expression. Data are means±S.D. *P<0.02 compared with sinus rhythm patients.

mechanism of AF in human tissues is extremely complex, because atrial remodeling consists of electrical, contractile, and structural remodeling. In addition, structural remodeling may occur from chronic hemodynamic, metabolic, or inflammatory stressors. Many factors such as ion channels, proteins influencing calcium homeostasis, connexins, autonomic innervation, fibrosis, paracrine factors, and cytokines may be involved in the molecular mechanism of AF. The present study using oligonucleotide microarray analysis demonstrated that about one hundred genes were modulated in the right atrium of patients with AF. These findings suggest that these genes may play critical roles in the initiation or perpetuation of AF and the pathophysiology of atrial remodeling.

In the present study, DNA microarray analysis identified 33 AF-specific genes. Some of these genes encode NF-IL6-beta, macrophage migration inhibitory factor, A-raf-1 oncogene, vascular endothelial growth factor B, RhoC, and glutathione peroxidase. NF-IL6-beta mRNA expression induced in the atria of AF patients was confirmed by the real-time PCR method. NF-IL6-beta and macrophage migration inhibitory factor are involved in inflammation [19,21]. Chung et al. [20] reported that C-reactive protein, a marker of systemic inflammation, is elevated in AF patients compared with sinus rhythm patients. Novel and inflammatory mechanisms may promote the persistence of AF, potentially by inducing structural and/or electrical remodeling of the atria. A-raf-1 protooncogene encodes cytoplasmic protein serine/threonine kinase, which plays an important role in cell growth and development [22]. Vascular endothelial growth factor B with structural similarities to vascular endothelial growth factor and placenta growth factor has a role in angiogenesis and endothelial cell growth [23]. RhoC, small guanosine triphosphatase Rho, which regulates remodeling of the actin cytoskeleton during cell morphogenesis and motility [24], may contribute to the structural remodeling. Baumer et al. [25] demonstrated that the activity, mRNA, and protein levels of glutathione peroxidase, an antioxidative enzyme, decreased in human failing myocardium. However, the present study showed that the glutathione peroxidase mRNA level in AF patients was elevated.

The present study demonstrated that the expression of 63 genes in AF patients was significantly lower compared with sinus rhythm. For example, genes for sarcoplasmic reticulum Ca^{2+}ATPase 2 and connexin 43 in AF patients were downregulated. In the real-time PCR analysis, sarcoplasmic reticulum Ca^{2+}-ATPase 2 mRNA expression in the AF group was lower compared with that in the sinus rhythm group, but not significantly. Ohkusa et al. [26] also reported that sarcoplasmic reticulum Ca^{2+}-ATPase 2 mRNA in both the right and left atrial myocardial tissues from 13 patients with AF were significantly lower than in the right atrium of patients with sinus rhythm. A decrease in sarcoplasmic reticulum Ca^{2+}-ATPase 2 in the atria may sustain abnormal intracellular Ca^{2+} handling and changes in the electrophysiologic properties of atrial tissue, leading to the perpetuation of AF. Connexin 43 is one of the gap junctions that are clusters of closely packed channels. Gap junctions directly connect the cytoplasmic compartments of neighboring cells and allow the passage of ions and small molecules. In the present study, connexin 43 mRNA expression in AF patients was downregulated. It is still controversial whether connexin 43 is upregulated [27], unchanged or downregulated in AF. Thus, changes in the expressions of connexin 43 might affect conduction velocity, contributing to sustained AF.

Previous studies demonstrated that some genes including L-type calcium channel [28], potassium channels [29], and sarcoplasmic reticulum Ca^{2+}-ATPase 2 [26,28] are modulated in AF patients. However, the molecular

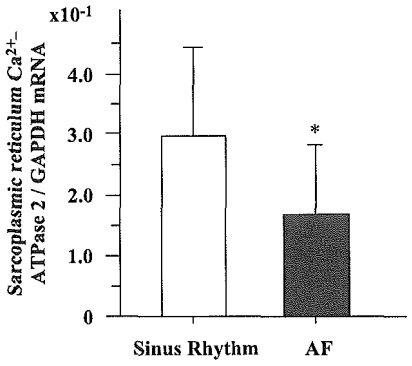

Fig. 2. Sarcoplasmic reticulum Ca^{2+}-ATPase 2 mRNA expression in the right atria of patients with sinus rhythm and atrial fibrillation (AF). Total RNA obtained from the right atria of patients with sinus rhythm (n=10) and AF (n=7) using RNAzol B (TEL-TEST) was analyzed by quantitative real-time reverse transcription-PCR as described in Methods. The amount of mRNA expression for sarcoplasmic reticulum Ca^{2+}-ATPase 2 was standardized to that of glyceraldehyde-3 phosphate dehydrogenase (GAPDH) mRNA expression. Data are means±S.D. *P<0.1 compared with sinus rhythm patients.

mechanism of AF is poorly understood. Although the roles of other genes including ESTs in the heart except for the genes described above still remain unknown, the genes screened in this study may provide insights into the initiation or perpetuation of AF and the pathophysiology of atrial remodeling, because DNA microarray is a highly effective method for screening genes.

Acknowledgements

This study was supported by grants from the Ministry of Education, Science, Sports and Culture of Japan (15590769), Tokyo, Japan, the Mitsui Life Social Welfare Foundation, Tokyo, Japan, the Takeda Science Foundation, Osaka, Japan, the Daiwa Securities Health Foundation, Tokyo, Japan, and the Sankyo Foundation of Life Science, Tokyo, Japan.

References

[1] Cerebral Embolism Task Force. Cardiogenic brain embolism. Arch Neurol 1986;43:71–84.
[2] Wolf PA, Dawber TR, Thomas Jr HE, Kannel WB. Epidemiologic assessment of chronic atrial fibrillation and risk of stroke: the Framingham study. Neurology 1978;28:973–7.
[3] Okishige K, Sasano T, Yano K, Azegami K, Suzuki K, Itoh K. Serious arrhythmias in patients with apical hypertrophic cardiomyopathy. Intern Med 2001;40:396–402.
[4] Redfield MM, Kay GN, Jenkins LS, Mianulli M, Jensen DN, Ellenbogen KA. Tachycardia-related cardiomyopathy: a common cause of ventricular dysfunction in patients with atrial fibrillation referred for atrioventricular ablation. Mayo Clin Proc 2000;75:790–5.
[5] Iyer VR, Eisen MB, Ross DT, et al. The transcriptional program in the response of human fibroblasts to serum. Science 1999;283:83–7.
[6] Feng Y, Yang JH, Huang H, et al. Transcriptional profile of mechanically induced genes in human vascular smooth muscle cells. Circ Res 1999;85:1118–23.
[7] Stanton LW, Garrard LJ, Damm D, et al. Altered patterns of gene expression in response to myocardial infarction. Circ Res 2000;86:939–45.
[8] Friddle CJ, Koga T, Rubin EM, Bristow J. Expression profiling reveals distinct sets of genes altered during induction and regression of cardiac hypertrophy. Proc Natl Acad Sci U S A 2000;97:6745–50.
[9] Yang J, Moravec CS, Sussman MA, et al. Decreased SLIM1 expression and increased gelsolin expression in failing human hearts measured by high-density oligonucleotide arrays. Circulation 2000;102:3046–52.
[10] Greene DG, Carlisle R, Grant C, Bunnell IL. Estimation of left ventricular volume by one-plane cineangiography. Circulation 1967;35:61–9.
[11] Sellers RD, Levy MJ, Amplatz K, Lillehei CW. Left retrograde cardioangiography in acquired cardiac disease: technic, indications and interpretation in 700 cases. Am J Cardiol 1964;14:437–47.
[12] Sahn DJ, DeMaria A, Kisslo J, Weyman A. Recommendations regarding quantitation in M-mode echocardiography: results of a survey of echocardiographic measurements. Circulation 1978;58: 1072–1083.
[13] Miyatake K, Okamoto M, Kinoshita N, et al. Evaluation of tricuspid regurgitation by pulsed Doppler and two-dimensional echocardiography. Circulation 1982;66:777–89.
[14] Lockhart DJ, Dong H, Byrne MC, et al. Expression monitoring by hybridization to high-density oligonucleotide arrays. Nat Biotechnol 1996;14:1675–80.
[15] Lee CK, Klopp RG, Weindruch R, Prolla TA. Gene expression profile of aging and its retardation by caloric restriction. Science 1999; 285:1390–3.
[16] Golub TR, Slonim DK, Tamayo P, et al. Molecular classification of cancer: class discovery and class prediction by gene expression monitoring. Science 1999;286:531–7.
[17] Heid CA, Stevens J, Livak KJ, Williams PM. Real time quantitative PCR. Genome Res 1996;6:986–94.
[18] Kruse N, Pette M, Toyka K, Rieckmann P. Quantification of cytokine mRNA expression by RT PCR in samples of previously frozen blood. J Immunol Methods 1997;210:195–203.
[19] Kinoshita S, Akira S, Kishimoto T. A member of the C/EBP family, NF-IL6 beta, forms a heterodimer and transcriptionally synergizes with NF-IL6. Proc Natl Acad Sci U S A 1992;89:1473–6.
[20] Chung MK, Martin DO, Sprecher D, et al. C-reactive protein elevation in patients with atrial arrhythmias: inflammatory mechanisms and persistence of atrial fibrillation. Circulation 2001;104:2886–91.
[21] Bacher M, Metz CN, Calandra T, et al. An essential regulatory role for macrophage migration inhibitory factor in T-cell activation. Proc Natl Acad Sci U S A 1996;93:7849–54.
[22] Lee JE, Beck TW, Brennscheidt U, DeGennaro LJ, Rapp UR. The complete sequence and promoter activity of the human A-raf-1 gene (ARAF1). Genomics 1994;20:43–55.
[23] Olofsson B, Pajusola K, Kaipainen A, et al. Vascular endothelial growth factor B, a novel growth factor for endothelial cells. Proc Natl Acad Sci U S A 1996;93:2576–81.
[24] Maekawa M, Ishizaki T, Boku S, et al. Signaling from Rho to the actin cytoskeleton through protein kinases ROCK and LIM-kinase. Science 1999;285:895–8.
[25] Baumer AT, Flesch M, Wang X, Shen Q, Feuerstein GZ, Bohm M. Antioxidative enzymes in human hearts with idiopathic dilated cardiomyopathy. J Mol Cell Cardiol 2000;32:121–30.
[26] Ohkusa T, Ueyama T, Yamada J, et al. Alterations in cardiac sarcoplasmic reticulum Ca^{2+} regulatory proteins in the atrial tissue of patients with chronic atrial fibrillation. J Am Coll Cardiol 1999;34:255–63.
[27] van der Velden HM, Ausma J, Rook MB, et al. Gap junctional remodeling in relation to stabilization of atrial fibrillation in the goat. Cardiovasc Res 2000;46:476–86.
[28] Brundel BJ, van Gelder IC, Henning RH, et al. Gene expression of proteins influencing the calcium homeostasis in patients with persistent and paroxysmal atrial fibrillation. Cardiovasc Res 1999;42:443–54.
[29] Brundel BJ, VanGelder IC, Henning RH, et al. Alterations in potassium channel gene expression in atria of patients with persistent and paroxysmal atrial fibrillation: differential regulation of protein and mRNA levels for K+channels. J Am Coll Cardiol 2001;37:926–32.

CMLS, Cell. Mol. Life Sci. 62 (2005) 2140–2146
1420-682X/05/182140-7
DOI 10.1007/s00018-005-5270-5

CMLS Cellular and Molecular Life Sciences

Research Article

Regulation of *Amh* during sex determination in chickens: *Sox* gene expression in male and female gonads

S. Takada[a, b], H. Mano[b] and P. Koopman[a, *]

[a] Institute for Molecular Bioscience, The University of Queensland, Brisbane, Queensland 4072 (Australia), Fax: +61 7 3346 2101, e-mail: p.koopman@imb.uq.edu.au
[b] Division of Functional Genomics, Jichi Medical School, 3311-1 Yakushiji, Minamikawachimachi, Kawachigun, Tochigi 329-0498 (Japan)

Received 18 June 2005; received after revision 22 June 2005; accepted 27 June 2005
Online First 26 August 2005

Abstract. During mammalian sexual development, the SOX9 transcription factor up-regulates expression of the gene encoding anti-Müllerian hormone (AMH), but in chickens, *Sox9* gene expression reportedly occurs after the onset of Amh expression. Here, we examined expression of the related gene *Sox8* in chicken embryonic gonads during the sex-determining period. We found that *cSox8* is expressed at similar levels in both sexes at embryonic day 6 and 7, and only at the anterior tip of the gonad, suggesting that SOX8 is not responsible for the sex-specific increase in *cAmh* gene expression at these stages. We also found that several other chicken *Sox* genes (*cSox3*, *cSox4* and *cSox11*) are expressed in embryonic gonads, but at similar levels in both sexes. Our data suggest that the molecular mechanisms involved in the regulation of *Amh* genes of mouse and chicken are not conserved, despite similar patterns of *Amh* expression in both species.

Key words. Sex determination; Amh; chicken; testis.

Even though molecular mechanisms of patterning and morphogenesis are surprisingly well conserved during metazoan evolution, mechanisms governing sex determination and gonadal development are diverse, even among vertebrates. In mammals, the heterogametic pairing of sex chromosomes (XY) results in male development. The mouse and human sex-determining gene, *Sry/SRY* (sex-determining region on Y chromosome), has been identified [1, 2] and is known to cause the bipotential gonad to differentiate into a testis [3]. However, *Sry* is not a conserved sex-determining gene as it exists only in mammals [4–7]. In contrast to mammals, in birds males are homogametic (ZZ) and females are heterogametic for the sex chromosomes (ZW). Whether avian sex is determined by a master female-determining gene on the W chromosome or by Z chromosome gene dosage is still unclear [8].

There are reports for the mouse that several genes are expressed predominantly in the developing testis but not in the ovary and, therefore, are likely to be important for male sex determination and differentiation. Some of these genes, such as *Amh* (anti-Müllerian hormone) and *Sox9* [9–12] are expressed similarly in mouse and chicken gonads, suggesting that there could be some degree of similarity between the molecular pathways and sexual development in chicken and mouse. However, some differences are evident. For example, *Sf1* (steroidogenic factor 1) and *Gata4* are predominantly expressed in the male gonad in mice [13, 14], while in chicken expression levels of both genes are similar between male and female gonads [12, 15].

* Corresponding author.

Sox genes represent a family related by the *Sry*-type high-mobility group (HMG) box, and function as transcription factors in various developmental processes through binding to a conserved core DNA sequence [16]. Twenty *Sox* genes have been identified in mouse and human, and are classified by their HMG box sequences into subgroups A–H [17, 18]. The expression pattern of each gene tends to be conserved in mouse and chicken. Among them, *Sox9* (group E) is known to act as a sex-determining gene. Mutations of human *SOX9* cause campomelic dysplasia, a severe skeletal malformation syndrome associated in most cases with XY sex reversal [19, 20], and ectopic expression of *Sox9* in XX mouse fetal gonads induces testis formation [21].

AMH plays an important role in inducing the regression of the Müllerian ducts in males, which normally give rise to the uterus, oviducts, upper vagina and fallopian tubes in females [22]. Analysis of mouse and human *Amh* gene regulation has uncovered several factors important for modulating *Amh* expression. For example, SF1 up-regulates *Amh* expression by cooperative interaction with WT1 [23], GATA-4 [24], SOX9 [25] and SOX8 [26]. Mice mutant for the SOX-binding site or the SF1-binding site in the *Amh* promoter revealed that SOX proteins are essential for *Amh* expression, while SF1 enhances the final expression level [27]. Oréal et al. [28] were the first to describe the chicken *Amh* promoter and showed that it has little overall homology with the mouse *Amh* promoter, but contains two putative SOX-binding sites and one SF1-binding site, suggesting that the mouse and chicken *Amh* promoters are similarly regulated. However, chicken *Sox9* is expressed too late to be a *cAmh* regulator [28, 29], but another SOX protein might substitute for SOX9 and, together with SF1, regulate *cAmh* expression.

Previously, we hypothesized that SOX8 might be a candidate transcription factor for regulating the chicken *Amh* gene [26, 30]. Mouse *Sox8* is expressed male specifically during gonad development. Its expression starts prior to the onset of *Amh* gene expression, and encodes a protein product that can up-regulate mouse *Amh* together with SF1 in vitro [26]. Group E Sox genes, consisting of Sox8, Sox9 and Sox10, show moderate levels of amino acid similarity and have similar genomic organization, suggesting that group E *Sox* genes may originate from one ancestral gene [31]. Although expression patterns of *Sox9* and *Sox10* overlap to a limited extent [32, 33], expression of *Sox8* overlaps substantially with expression of *Sox9* [31, 32] and to a lesser extent, *Sox10* [33, 31]. This fact suggests that there is some functional redundancy between SOX8 and SOX9, similar to that published for SOX1, SOX2 and SOX3 in lens formation [34], L-SOX5 and SOX6 in cartilage formation [35] and SOX7, SOX17 and SOX18 in vasculogenesis [36–38].

In this study, we analyzed the expression patterns of chicken *Sox8* in developing gonads during the sex-determining window. If *cSox8* contributes to *cAmh* gene expression, one would expect to find *cSox8* predominantly expressed in the embryonic testis and prior to the onset of *cAmh*. We found this not to be the case, suggesting that SOX8 is not responsible for sex-specific expression of *cAmh* in chicken. We also tested the expression patterns of several other *cSox* genes which are expressed in embryonic testis, and similarly found that they were not expressed male specifically.

Materials and methods

Chicken embryos. Fertilized chicken eggs were obtained from local suppliers (Ingham, Brisbane, Australia and Saitama Experimental Animal Supply, Saitama, Japan) and maintained at 18 °C until use. Eggs were transferred to an incubator at 37.5 °C and allowed to develop for 5, 6 or 7 days. Staging was confirmed at dissection according to Hamburger and Hamilton [39]. The entire urogenital ridge of each embryo was explanted for whole-mount *in situ* hybridization. Sexing was performed by PCR as described elsewhere [40] using genomic DNA purified from a hind limb of each embryo.

Amplification of HMG box sequences. Total RNA was isolated from left and right gonads of day 6 male embryos by standard methods [41]. RNA (0.5 μg) was then treated with DNaseI and first-strand cDNA was synthesized using M-MLV reverse transcriptase (Invitrogen) according to the manufacturer's protocol. For amplification of the HMG box, the PCR reaction was carried out in a solution containing 1 x NH_4 buffer (Bioline), 100 M $MgCl_2$, 100 μM dNTPs, 0.4 μM primers and 0.5 unit Biotaq DNA polymerase (Bioline) with 4.5 min denaturation at 95 °C followed by 40 cycles of amplification at 95 °C for 30 s and 57 °C for 30 s. The PCR product was cloned into pGEM-T Easy (Promega). Sequencing was performed using the BigDye Terminator v3.1 Cycle Sequencing Kit (Applied Biosystems) and M13 reverse primer, and electrophoresis was carried out by the Australian Genome Research Facility, Brisbane, Australia. Primer sequences used were as follows; G7A1: 5'-AGC G(A/G)C CCA TGA ACG C(A/C/G/T)T T-3' and G7B1: 5'-CGC (C/T)GG TA(C/T) TT(A/G) TA(A/G) TC(A/C) GGG T-3'. The PCR reaction was also carried out using genomic DNA as a template.

RT-PCR of *Sox* genes, *Amh* and *Actin*. The left and right gonads of staged, sexed embryos were pooled (ten and five embryos of each sex for day 6 and day 7, respectively) to isolate total RNA using the RNeasy Mini kit (Qiagen) with the optional on-column DNase digestion with the RNase-free DNase set. The first-strand cDNA was synthesized from 1 μg of total RNA using Power-

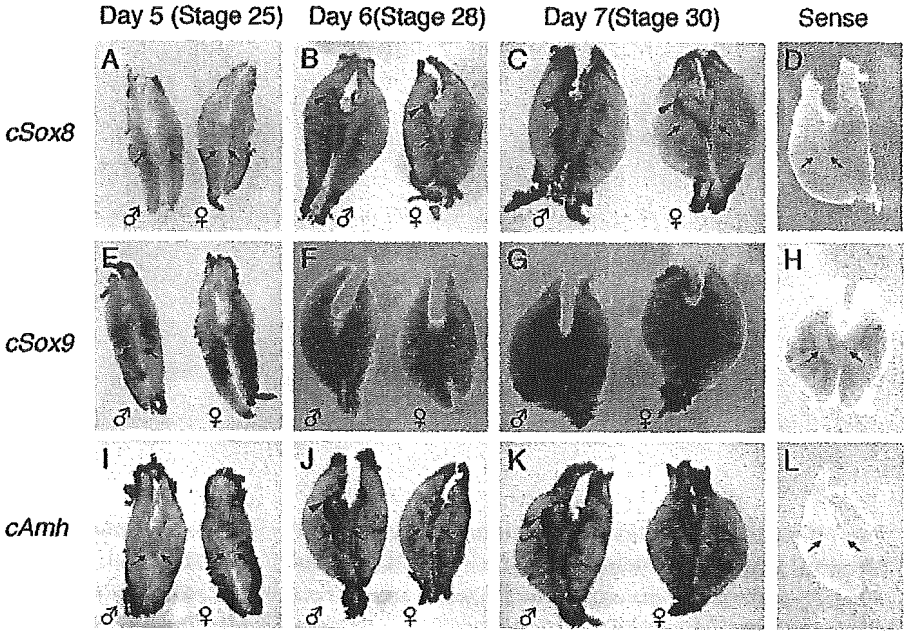

Figure 1. Whole-mount *in situ* hybridization of *cSox8*, *cSox9* and *cAmh* in the chicken embryonic gonad/mesonephros. In each panel, male (♂) and female (♀) gonad/mesonephros are left and right, respectively. Probes used are shown at the left of each panel. The samples in A–C, E–G and I–K were hybridized with antisense probe. In D and L a day 6 sample hybridized with sense probe. In H a day 7 sample was hybridized with sense probe. Developmental stages (days and Hamburger-Hamilton stage) of gonad/mesonephros are labeled above. Arrow shows the position of gonad. Arrowheads point to regions of positive staining.

Script reverse transcriptase (Clontech) and oligodT. PCR amplification was carried out using the QuantiTect SYBR Green PCR kit (Qiagen) with uracil-N-glycosylase and the 7900HT Sequence Detection System (Applied Biosystems). Samples were incubated at 50 °C for 2 min, then 95 °C for 15 min, followed by 40 cycles of amplification at 94 °C for 30 s, 54.2 °C for 1 min and 72 °C for 1 min. For the amplification of *cSox8* and *cSox9*, 85.4 °C for 15sec was added after each 72 °C step of each amplification cycle. Primer sequences used were as follows; cSox3-1: 5'-GCACCAGCACTACCAGAG-3' and cSox3-2: 5'-CGA ATG CGG ACA CGA ACC) for *cSox3* [29], cSox4F: 5'-TCG GGG GAT TGG CTG GAG TC-3' and cSox4R: 5'- CTC AGC CGA TCC TCG TTT CC-3' for *cSox4*, cSox8RTF : 5'-CTA CAA GGC TGA CAG CGG GC-3' and cSox8RTR: 5'-AGG CCG GGC TCT TGT GAG TC-3' for *cSox8*, cSox9F: 5'-CCC CAA CGC CAT CTT CAA-3' and cSox9R: 5'-CTG CTG ATG CCG TAG GTA-3' for *cSox9*, cSox11F2: 5'-AAG CAG GAG GCG GAC GAC GA-3' and cSox11R2: 5'-CGC CCC GCA CCT CCT CGT AG-3' for *cSox11*, cAmh-1: 5'-GTG GAT GTG GCT CCC TAC CC-3' and cAmh-2: 5'-GCA GCA CCG AGG GCT CCT CC-3' for *cAmh* [29] and Actin-1: 5'-TGG ATG ATG ATA TTG CTG C-3' and Actin-2: 5'-ATC TTC TCC ATA TCA TCC C-3' [29] for *Actin*. To calculate the relative amount of gene expression levels, the $\Delta\Delta C_T$ method was used. Three independent pooled samples were analyzed. Maximum average values were set as 100%.

For the RT-PCR amplification of *cSox12* and *cSox14*, the same cDNA for the real-time RT-PCR was used. The PCR reaction was carried out in the same solution as HMG box amplification with 4.5 min denaturation at 95 °C followed by 40 cycles of amplification at 95 °C for 30 s and 50 °C for 30 s. Primer sequences used were as follows; cSox12F: 5'-AGA TCT CCA AGC GCC TGG GTC G-3' and cSox12R: 5'-GGT AGT CGG CCA TGT GCT TG-3' for *cSox12*, cSox14F: 5'-GAG GTT CCT CAC ACC TTG GC-3' and cSox14R: 5'-ACA CGG AGG AAT CCC AGT CC-3' for *cSox14*.

Probes. The previously reported *cAmh* probe [9] was obtained by RT-PCR amplification of an 821-bp fragment, using primers cAMHRTF (5'-ACG GTG CGC GCC CAC TGG CAG G-3') and cAMHRTR (5'-ACG TCG TGA CCT GCA AGC CCT C-3') and RNA prepared from 5.5-day-old whole embryo. The *cSox8* probe was cloned by PCR using primers chSox8C2F (5'-CTG CAG AGC TCC AAC TAC TAC A-3') and chSox8C2R (5'-GAG CTC TGT CCT TTT GGA GAG T-3') and chicken genomic DNA as the template. The fragment corresponds to nucleotides 1228–1589 of the *cSox8* mRNA sequence (accession No. AF228664). PCR products of *cAmh* and *cSox8* were cloned into the pGEM-T Easy vector. The *cSox9* probe was reported previously by Kent et al. [11]. The *cSox11* fragment was cloned by SacI digestion of *cSox11* cDNA and subsequent insertion into pBluescriptII KS vector. The fragment corresponds to nucleotides 667–967 of the *cSox11* mRNA sequence (accession No. AB012237). The *cSox4* probe was obtained by KspI digestion of *cSox4* cDNA and subsequent insertion into pBluescriptII KS vector. The fragment corresponds to nucleotides 576–965 of the chicken *Sox4* mRNA sequence (accession No. AY493693).

***In situ* hybridization.** Sense and antisense digoxygenin-labeled RNA probes were generated by *in vitro* transcrip-

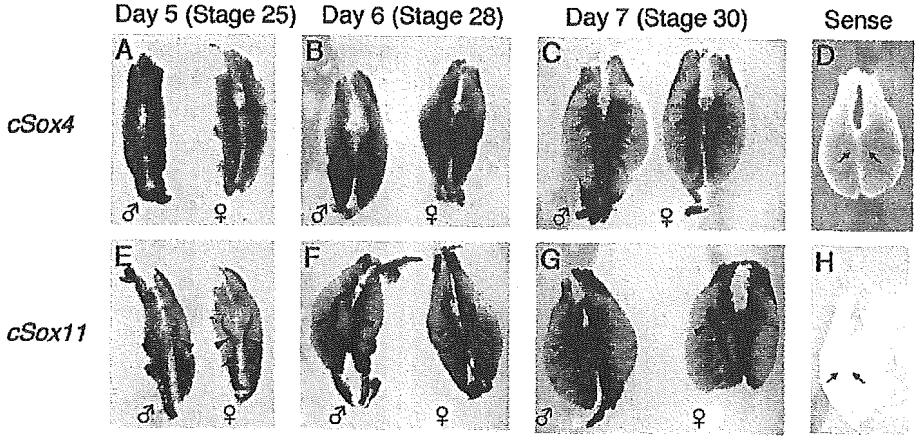

Figure 2. Whole-mount *in situ* hybridization of *cSox4* and *cSox11* in the chicken embryonic gonad/mesonephros. In each panel, male (♂) and female (♀) gonad/mesonephros are left and right, respectively. Probes used are shown at the left of each panel. A–C and E–G were hybridized with antisense probe. D and H show day 6 samples hybridized with sense probe. Developmental stages (days and Hamburger-Hamilton stage) of gonad/mesonephros are labeled above. Arrow shows the position of gonad. Arrowheads point to regions of staining.

tion. Whole mount *in situ* hybridization was performed as described using the maleic acid buffer (MABT) method [42]. Experiments were carried out at least twice for each probe, with similar results.

Results and discussion

To compare the temporospatial expression of *cSox8* and *cAmh* in embryonic gonads, we employed whole-mount *in situ* hybridization analysis using female and male gonad/mesonephros complexes isolated from day 5, 6 and 7 chicken embryos (Hamburger and Hamilton stages 25, 28 and 30, respectively [39]). These stages cover the temporal window at which sexual dimorphism in the gonad first becomes apparent [43]. In addition to providing spatial information relating to gene expression, whole-mount *in situ* hybridization is commonly used as a semiquantitative guide to gene expression levels between different tissues hybridized with the same probe and incubated under the same conditions, as in the experiments described below.

As expected, *cAmh* was expressed at higher levels in male than in female gonads at day 6 and 7 (fig. 1J, K). Expression levels in the right male gonads were higher than in the left, possibly reflecting the asymmetric development of avian genital ridges [43]. We did not observe expression of *cAmh* at day 5 (fig. 1I), even though Oréal et al. [28] reported that *cAmh* is expressed weakly and at similar levels in male and female gonads at day 5 by section *in situ* hybridization. This may reflect lower sensitivity of our whole mount *in situ* hybridization method.

Previous workers have reported that male-specific high-level expression of *cSox9* is preceded by expression of *cAmh* in the chick [28, 29]. We analyzed the temporal expression of *cSox9* in chicken embryos. No signal was observed in male or female gonads at day 5 or day 6 (fig. 1E, F). High levels of *cSox9* expression were observed in day 7 male gonads, while no signal was observed in the day 7 female (fig. 1G). This compares to the results of Oréal et al. [28] who described very faint expression of *cSox9* in day 6 gonads by *in situ* hybridization using sections. Our data demonstrate high levels of *cAmh* expression in day 6 male gonad, preceding the high levels of *cSox9* expression first detected in day 7 male gonad. They suggest that SOX9 is not responsible for the male-specific up-regulation of *cAmh*, but may play a role in the maintenance and/or amplification of *cAmh* expression in the male gonads once transcription is initiated. Our results support the previous observation that the male-specific high levels of *cAmh* expression precede testicular *cSox9* expression [28, 29].

We next examined expression of *Sox8*. At day 5, no *cSox8* expression was observed (fig. 1A). At day 6 and 7, *cSox8* expression was observed at the anterior tip of both male and female right gonads at similar levels (fig. 1B, C). This expression profile is different from that of *cAmh*, both in spatial distribution of transcripts and degree of sex specificity, suggesting that SOX8 could not be responsible for sex-specific up-regulation of *cAmh* in chicken.

The expression patterns of mouse and chicken *Sox8* imply that the functions of SOX8 are conserved in most but not all tissues between the two species. For example, *Sox8* is expressed in brain, skeletal muscle, eye, somite, dermomyotome, limb, digits, gut, spinal cord and dorsal root ganglia in both species [30, 31, 44]. However, some differences are evident in embryonic heart and gonad: in chicken, *cSox8* is expressed in the embryonic heart, testis and ovary, whereas in mouse, *Sox8* expression occurs predominantly in the embryonic testis, but not in the ovary or heart [31, 44]. Given these observations, SOX8 may contribute to the male-specific activation of *Amh* expression during gonadgenesis in mice but not chicken.

In mouse, only two SOX proteins, SOX8 and SOX9, have been identified as regulators of *Amh* expression in the embryonic gonad [26]. Based on our data, and previous studies [28, 29], neither SOX8 nor SOX9 can be responsible for the onset of high levels of *cAmh* expression

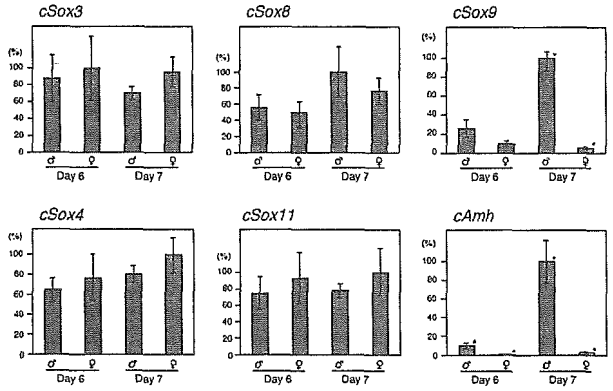

Figure 3. Quantitative, real-time RT-PCR analysis of *Sox* and *Amh* gene expression. Averages of three independent trials are shown as bars, with SEs shown as lines. Values marked with * were significantly different between males (♂) and females (♀) ($p = 0.0017$, 0.0047 and 0.012 for cSox9 at day 7, cAmh at day 6 and 7, respectively, using a two-sample equal variance t-test). Others were not significantly different between males and females ($p = 0.81$, 0.24, 0.74, 0.52, 0.17, 0.67, 0.38, 0.64, 0.49 for *cSox3* at day 6 and 7, *cSox8* at day 6 and 7, *cSox9* at day 6, *cSox4* at day 6 and 7, and *cSox11* at day 6 and 7, respectively).

in chicken, even though two SOX-binding sites are predicted in the *cAmh* promoter region. These observations prompted us to search for other *Sox* genes expressed in chicken male gonads that could be considered as candidate regulators of *Amh* expression. We conducted the analysis at day 6, since at this stage *cAmh* is expressed at high levels in male gonads while *cSox9* is either not expressed or expressed at a very low level.

We utilized degenerate RT-PCR on purified day 6 male gonad RNA using generic *Sry*-type HMG box primers to generate fragments for cloning into a plasmid vector. Twenty independent clones were sequenced, revealing that 12 clones were *cSox4* [45], 7 were *cSox11* [46] and 1 was *cSox9* [47].

One possible explanation for these results is that the degenerate primers used show a bias for amplification of *cSox4* and *cSox11* templates. To examine this possibility, we used the same degenerate primers to amplify *Sox* fragments from genomic DNA, in which all intronless *Sox* genes (Sox1, -2, -3, -4, -11, -12, -14, -21) capable of amplification by the primers are represented in equal proportions. Among ten clones amplified, none was *cSox4* or *cSox11*. Thus, primer bias does not explain our data relating to *cSox4* and *cSox11* expression in developing chicken gonads.

cSox4 and *cSox11* are expressed in male gonads at day 6, prompting us to examine the expression profiles of each in male and female gonads through the sex determination window. If both or either is expressed preferentially in male gonads, they could be considered a candidate for regulation of the *cAmh* gene. To evaluate the expression patterns of *cSox4* and *cSox11* in embryonic gonads, we employed whole-mount *in situ* hybridization analysis at the same stages previously used to profile *cSox8*, *cSox9* and *cAmh* expression. *cSox4* and *cSox11* signals were detected at similar levels in male and female gonads at all stages examined (fig. 2) suggesting that neither of them plays a role in sex-specific regulation of *Amh*.

The identification of *Sox* genes that are expressed in chicken embryonic gonads at day 5, 6 and 7 was previously attempted by McBride et al. [6]. Using RT-PCR amplification of the conserved *Sry*-type HMG box domain from RNA samples prepared from testes with mesonephroi attached, they found expression of *cSox3*, *cSox4*, *cSox9*, *cSox11*, *cSox12* and *cSox14*. Our data confirm that *cSox4*, *cSox9* and *cSox11* are indeed expressed, as is cSox3 (see below); however; we amplified the HMG box from day 6 gonad only, and this difference along with the differences in PCR primers, may explain the discrepancies in the data for *cSox12* and *cSox14*. Moreover, day 6 male gonad expresses *cSox4* and *cSox11* transcripts so abundantly that RT-PCR cloning is difficult for *Sox* genes expressed at low levels.

To examine the levels of gene expression quantitatively, we utilized RT-PCR and real-time RT-PCR analyses using RNAs isolated from pooled, sexed embryonic gonads at days 6 and 7 (fig. 3). As expected, *cAmh* and *cSox9* were expressed at different levels between males and females at day 7. At day 6, the expression levels of *cAmh* were statistically different between males and females ($p < 0.005$) while the expression levels of *cSox9* were not ($p > 0.1$). However, *cSox3*, *cSox4*, *cSox8* and *cSox11* were expressed at similar levels between males and females at days 6 and 7, suggesting that none of these *Sox* genes is responsible for the male-specific up-regulation of *cAmh* expression.

We were unable to amplify *cSox12* and *cSox14* sequences by RT-PCR from chicken embryonic gonads. As a positive control, chicken genomic DNA was included as template. Signals were observed at expected size of 108 bp for *cSox12* and 331 bp for *cSox14* only from genome template, but not from gonad RNA samples, showing that neither gene is expressed in embryonic gonads at day 6 and day 7 (data not shown).

Previous studies have eliminated *cSox3* as a candidate for male-specific up-regulation of *Amh* expression because *cSox3* is expressed at similar levels in the male and female gonads at the sex-determining window [28, 29]. Our present data support this conclusion. We rule out *cSox8* because it is expressed in a different spatial pattern to *Amh*, and *cSox12* and *-14* because they are not expressed in gonads at sex-determining stages at all. We exclude *cSox4* and *cSox11* also, on the basis of equivalent expression levels between male and female. It is formally possible that *cSox4* and *cSox11* might be expressed in Sertoli cells in the male (the site of *Amh* expression) and in another cell lineage in females, in which *Amh* is

not expressed, but we consider this unlikely, especially considering that all genes found to be involved in sex-specific development of the gonads to date show a sexually dimorphic pattern of gene expression in fetal gonads when examined by whole-mount *in situ* hybridization. However, one still cannot exclude the possibility of SOX protein-mediated regulation of *cAmh* gene expression, and further extensive cloning of *cSox* genes may be necessary to discover a *Sox* gene expressed predominantly in chicken embryonic testis.

Alternatively, we have to consider that sex-specific *Amh* up-regulation is not mediated by SOX proteins in birds. Even though the putative SF1-binding site, like the two SOX-binding site in the *Amh* promoter, is conserved between mouse and chicken [28], and *cSf1* is co-expressed with *cAmh* at day 7 of chicken embryonic testis [15], the expression profiles of mouse and chicken *Sf1* show major differences. Before testis cord formation, *Sf1* is expressed at similar levels in males and females in both species, while subsequently, chicken *Sf1* expression is maintained in the testis, but is up-regulated in the ovary [12, 15, 29]. The opposite expression pattern is reported for mouse *Sf1* [reviewed in ref. 48]. This difference could be explained by the possibility that *SF1* functions in more steroidogenically active tissue (testis in mammals and ovary in birds), or that *Sf1* may not be associated with testis formation in birds [12]. Either way, the expression profile of *cSf1*, like that of *cSox9* [28] and *cSox8* (this study), suggests that it is not responsible for male-specific up-regulation of *cAmh* expression during chicken gonad genesis. Since both SF1 and SOX proteins are required for normal levels of *Amh* expression during sex determination in mouse [27], this may imply that there is a different mechanism of *cAmh* regulation in chicken compared with mouse, and that SOX protein is not a causative factor for sex-specific expression of *cAmh*.

Gonadal expression of *Sox8*, which has an evolutionarily conserved coding protein among vertebrates, has been studied in mouse, chicken and red-eared slider turtle [31, 49]. *Sox8* is expressed in the developing testes of all three species, implying a functional significance, but in chicken and turtle, *Sox8* is also expressed in the ovary. So far, up-regulation of mouse *Amh* is the only known molecular function for the SOX8 protein [26]. If this function is conserved among vertebrates, chicken SOX8 may have a protein partner which is expressed in males to activate or in females to suppress *cAmh*. Some genes are expressed sex specifically during gonadal differentiation in the mouse, including *Sf1* [13], *Wt1* [50], *Gata4* [14], *Lhx9* [51], *Wnt-4* [52] and *Dax1* [53]. However, chicken homologues of these genes are not candidates because they are expressed in both developing testis and ovary while *cAmh* is differentially expressed [15, 29]. *Dmrt1* is expressed only in developing testis in mouse, while chicken *Dmrt1* is expressed in both developing gonads with higher levels in testis, suggesting that it is not such a factor [15, 54]. The identification of a chicken SOX8-binding partner may clarify this possibility. Finally, further analysis of the *cAmh* promoter may reveal whether SOX proteins play a role in its up-regulation, and whether similarities exist in the mechanisms that regulate *Amh* expression in birds and mammals.

Acknowledgements. We thank M. Hargrave, K. Loffler and J. Bowles and members of the Koopman laboratory for technical advice and constructive criticism, and D. Wilhelm and F. Martinson for critical reading of this manuscript. P. K. is a Professorial Research Fellow of the Australian Research Council.

1 Gubbay J., Collignon J., Koopman P., Capel B., Economou A., Münsterberg A. et al. (1990) A gene mapping to the sex-determining region of the mouse Y chromosome is a member of a novel family of embryonically expressed genes. Nature **346:** 245–250
2 Sinclair A. H., Berta P., Palmer M. S., Hawkins J. R., Griffiths B. L., Smith M. J. et al. (1990) A gene from the human sex-determining region encodes a protein with homology to a conserved DNA-binding motif. Nature **346:** 240–244
3 Koopman P., Gubbay J., Vivian N., Goodfellow P. and Lovell-Badge R. (1991) Male development of chromosomally female mice transgenic for Sry. Nature **351:** 117–121
4 Coriat A.-M., Muller U., Harry J. L., Uwanogho D. and Sharpe P. T. (1993) PCR amplification of SRY-related gene sequences reveals evolutionary conservation of SRY-box Motif. PCR Methods Appl. **2:** 218–222
5 Griffiths R. (1991) The isolation of conserved DNA sequences related to the human sex determing region Y gene from the lesser black-backed gull (Larus fuscus). Proc. R. Soc. Lond. B. **224:** 123–128
6 McBride D., Sang H. and Clinton M. (1997) Expression of Sry-related genes in the developing genital ridge/mesonephros of the chick embryo. J. Reprod. Fertil. **109:** 59–63
7 Tiersch T. R., Mitchell M. J. and Wachtel S. S. (1991) Studies on the phylogenetic conservation of the SRY gene. Hum. Genet. **87:** 571–573
8 Clinton M. (1998) Sex determination and gonadal development: a bird's eye view. J. Exp. Zool. **281:** 457–465
9 Carré-Eusèbe D., Clemente N. di, Rey R., Pieau C., Vigier B., Josso N. et al. (1996) Cloning and expression of the chick anti-Müllerian hormone gene. J. Biol. Chem. **271:** 4798–4804
10 Morais da Silva S., Hacker A., Harley V., Goodfellow P., Swain A. and Lovell-Badge R. (1996) Sox9 expression during gonadal development implies a conserved role for the gene in testis differentiation in mammals and birds. Nat. Genet. **14:** 62–68
11 Kent J., Wheatley S. C., Andrews J. E., Sinclair A. H. and Koopman P. (1996) A male-specific role for SOX9 in vertebrate sex determination. Development **122:** 2813–2822
12 Smith C. A., Smith M. J. and Sinclair A. H. (1999b) Expression of chicken steroidogenic factor-1 during gonadal sex differentiation. Gen. Comp. Endocrinol. **113:** 187–196
13 Ikeda Y., Shen W. H., Ingraham H. A. and Parker K. L. (1994) Developmental expression of mouse steroidogenic factor-1, an essential regulator of the steroid hydroxylases. Mol. Endocrinol. **8:** 654–662
14 Viger R. S., Mertineit C., Trasler J. M. and Nemer M. (1998) Transcription factor GATA-4 is expressed in a sexually dimorphic pattern during mouse gonadal development and is a potent activator of the Müllerian inhibiting substance promoter. Development **125:** 2665–2675
15 Oréal E., Mazaud S., Picard J.-Y., Magre S. and Carré-Eusèbe D. (2002) Different patterns of anti-Müllerian hormone expres-

sion, as related to DMRT1, SF-1, WT1, GATA-4, Wnt-4, and Lhx9 expression, in the chick differentiating gonads. Dev. Dyn. **225:** 221–232
16 Wegner M. (1999) From head to toes: the multiple facets of Sox proteins. Nucleic Acids Res. **15:** 1409–1420
17 Bowles J., Schepers G. and Koopman P. (2000) Phylogeny of the SOX family of developmental transcription factors based on sequence and structural indicators. Dev. Biol. 227: 239–255
18 Schepers G. E., Teasdale R. D. and Koopman P. (2002) Twenty pairs of Sox: extent, homology, and nomenclature of the mouse and human sox transcription factor gene families. Dev. Cell. **3:** 167–170
19 Foster J. W., Dominguez-Steglich M. A., Guioli S., Kowk C., Weller P. A., Weissenbach J. et al. (1994) Campomelic dysplasia and autosomal sex reversal caused by mutations in an SRY-related gene. Nature **372:** 525–30
20 Wagner T., Wirth J., Meyer J., Zabel B., Held M., Zimmer J. et al. (1994) Autosomal sex reversal and campomelic dysplasia are caused by mutations in and around the SRY-related gene SOX9. Cell **79:** 1111–120
21 Vidal V. P. I., Chaboissier M.-C., Rooij D. G. de and Schedl A. (2001) Sox9 induces testis development in XX transgenic mice. Nat. Genet. **28:** 216–17
22 Josso N., Clemente N. di and Gouédard L. (2001) Anti-Müllerian hormone and its receptors. Mol. Cell. Endocrinol. **179:** 25–32
23 Nachtigal M. W., Hirokawa Y., Enyeart-VanHouten D. L., Flanagan J. N., Hammer G. D. and Ingraham H. A. (1998) Wilms' tumor 1 and Dax-1 modulate the orphan nuclear receptor SF-1 in sex-specific gene expression. Cell **93:** 445–454
24 Tremblay J. J. and Viger R. S. (1999) Transcription factor GATA-4 enhances Müllerian inhibiting substance gene transcription through a direct interaction with the nuclear receptor SF-1. Mol. Endocrinol. **13:** 1388–1401
25 Santa Barbara P. de, Bonneaud N., Boizet B., Desclozeaux M., Moniot B., Südbeck P. et al. (1998) Direct interaction of SRY-related protein SOX9 and steroidogenic factor 1 regulates transcription of the human anti-Müllerian hormone gene. Mol. Cell. Biol. **18:** 6653–6665
26 Schepers G., Wilson M., Wilhelm D. and Koopman P. (2003) SOX8 is expressed during testis differentiation in mice and synergizes with SF1 to activate the Amh promoter in vitro. J. Biol. Chem. **278:** 28101–28108
27 Arango N. A., Lovell-Badge R. and Behringer R. R. (1999) Targeted mutagenesis of the endogenous mouse Mis gene promoter: in vivo definition of genetic pathways of vertebrate sexual development. Cell **99:** 409–419
28 Oréal E., Pieau C., Mattei M. G., Josso N., Picard J.-Y., Carré-Eusèbe D. et al. (1998) Early expression of AMH in chicken embryonic gonads precedes testicular SOX9 expression. Dev. Dyn. **212:** 522–532
29 Smith C. A., Smith M. J. and Sinclair A. H. (1999a) Gene expression during gonadogenesis in the chicken embryo. Gene **234:** 395–402
30 Takada S. and Koopman P. (2003) Origin and possible roles of the Sox8 transcription factor gene during sexual development. Cytogenet. Genome Res. **101:** 212–218
31 Schepers G. E., Bullejos M., Hosking B. M. and Koopman P. (2000) Cloning and characterisation of the Sry-related transcription factor gene Sox8. Nucleic Acids Res. **28:** 1473–1480
32 Wright E., Hargrave M. R., Christiansen J., Cooper L., Kun J., Evans T. et al. (1995) The Sry-related gene Sox-9 is expressed during chondrogenesis in mouse embryos. Nat. Genet. **9:** 15–20
33 Pusch C., Hustert E., Pfeifer D., Südbeck P., Kist R., Roe B. et al. (1998) The SOX10/Sox10 gene from human and mouse: sequence, expression, and transactivation by the encoded HMG domain transcription factor. Hum. Genet. **103:** 115–123
34 Collignon J., Sockanathan S., Hacker A., Cohen-Tannoudji M., Norris D., Rastan S. et al. (1996) A comparison of the properties of Sox-3 with Sry and two related genes, Sox-1 and Sox-2. Development **122:** 509–520
35 Smits P., Li P., Mandel J., Zhang Z., Deng J. M., Behringer R. R. et al. (2001) The transcription factors L-Sox5 and Sox6 are essential for cartilage formation. Dev Cell **1:** 277–290
36 Downes M. and Koopman P. (2001) SOX18 and the transcriptional regulation of blood vessel development. Trends Cardiovasc. Med. **11:** 318–324
37 Kanai-Azuma M., Kanai Y., Gad J. M., Tajima Y., Taya C., Kurohmaru M. et al. (2002) Depletion of definitive gut endoderm in Sox17-null mutant mice. Development **129:** 2367–2379
38 Pennisi D., Bowles J., Nagy A., Muscat G. and Koopman P. (2000) Mice null for Sox18 are viable and display a mild coat defect. Mol. Cell. Biol. **20:** 9331–9336
39 Hamburger V. and Hamilton H. L-. (1951) A series of normal stages in the development of the chick embryo. J. Morphol. **88:** 49–92
40 Clinton M., Haines L., Belloir B. and McBride D. (2001) Sexing chick embryos: a rapid and simple protocol. Br. Poult. Sci. **42:** 134–138
41 Chomczynski P. and Sacchi N. (1987) Single-step method of RNA isolation by acid guanidinium thiocyanate-phenol-chloroform extraction. Anal. Biochem. **162:** 156–159
42 Xu Q. and Wilkinson D. (1998) In situ hybridization of mRNA with hapten labelled probes. In: In Situ Hybridization: a Practical Approach, 2nd ed., pp. 87–106, Wilkinson D. (ed.), Oxford University Press, Oxford
43 Romanoff A. L. (1960) The Avian Embryo: Structural and Functional Development, Macmillan, New York
44 Bell K. M., Western P. S. and Sinclair A. H. (2000) SOX8 expression during chick embryogenesis. Mech. Dev. 94: 257–260
45 Maschhoff K. L., Anziano P. Q., Ward P. and Baldwin H. S. (2003) Conservation of Sox4 gene structure and expression during chicken embryogenesis. Gene **320:** 23–30
46 Uwanogho D., Rex M., Cartwright E. J., Pearl G., Healy C., Scotting P. J. et al. (1995) Embryonic expression of the chicken Sox2, Sox3 and Sox11 genes suggests an interactive role in neuronal development. Mech. Dev. **49:** 23–36
47 Healy C, Uwanogho D. and Sharpe P. T. (1999) Regulation and role of Sox9 in cartilage formation. Dev. Dyn. **215:** 69–78
48 Parker K. L. and Schimmer B. P. (1997) Steroidogenic factor 1: a key determinant of endocrine development and function. Endocr. Rev. **18:** 361–377
49 Takada S., DiNapoli L., Capel B. and Koopman P. (2004) Sox8 is expressed at similar levels in gonads of both sexes during the sex determining period in turtles. Dev. Dyn. **231:** 387–395
50 Pelletier J., Schalling M., Buckler A. J., Rogers A., Haber D. A. and Housman D. (1991) Expression of the Wilms' tumor gene WT1 in the murine urogenital system. Genes. Dev. **5:** 1345–1356
51 Birk O. S., Casiano D. E., Wassif C. A., Cogliati T., Zhao L., Zhao Y. et al. (2000) The LIM homeobox gene Lhx9 is essential for mouse gonad formation. Nature **403:** 909–913
52 Vainio S., Heikkila M., Kispert A., Chin N. and McMahon A. P. (1999) Female development in mammals is regulated by Wnt-4 signalling. Nature **397:** 405–409
53 Swain A., Zanaria E., Hacker A., Lovell-Badge R. and Camerino G. (1996) Mouse Dax1 expression is consistent with a role in sex determination as well as in adrenal and hypothalamus function. Nat. Genet. **12:** 404–409
54 Raymond C. S., Kettlewell J. R., Hirsch B., Bardwell V. J. and Zarkower D. (1999) Expression of Dmrt1 in the genital ridge of mouse and chicken embryos suggests a role in vertebrate sexual development. Dev. Biol. **215:** 208–220

Available online at www.sciencedirect.com
SCIENCE DIRECT®
Journal of Steroid Biochemistry & Molecular Biology 96 (2005) 1–12
The Journal of Steroid Biochemistry & Molecular Biology
www.elsevier.com/locate/jsbmb

Transcriptional repression of fibroblast growth factor 8 by transforming growth factor-β in androgen-dependent SC-3 cells

Norio Takayashiki, Hirotoshi Kawata, Tomoko Kamiakito, Akira Tanaka *

Department of Pathology, Jichi Medical School, 3311-1 Yakushiji, Minamikawachi, Kawachi, Tochigi 329-0498, Japan

Received 5 July 2004; accepted 10 January 2005

Abstract

We here characterized the transcriptional profiles of TGF-β-responsive genes using androgen-dependent mouse mammary carcinoma SC-3 cells. Compared with the testosterone-stimulated SC-3 cells, 165 genes were up-regulated at more than 5-fold, and 78 genes were down-regulated to less than one-third in response to TGF-β. Of note, *fgf8*, an androgen-inducible growth factor essential to the androgen-dependent growth of SC-3 cells, was severely repressed in response to TGF-β. Real-time PCR confirmed that the androgenic induction of the *fgf8* transcripts is severely attenuated by TGF-β. Although a considerable number of growth-suppressive genes were up-regulated in response to TGF-β, the treatment with TGF-β was insufficient to lead SC-3 cells to apoptosis within 24 h by both the TUNEL method and the caspase 3 activity assay. Flow cytometric analysis rather indicated the cell-static effect of TGF-β on the androgen-stimulated SC-3 cells. In addition, TGF-β failed to suppress the FGF8-stimulated growth of SC-3 cells, suggesting that the repression of *fgf8* is required for the TGF-β-mediated growth inhibition in SC-3 cells. In a reporter assay, androgen-responsive promoter activity was suppressed by TGF-β in SC-3 cells. Based on this finding, it is likely that some of the androgen-inducible genes are physiological targets of the TGF-β-mediated transcriptional control, and therefore, it is strongly suggested that the repression of *fgf8* might be directly or indirectly involved in this transcriptional control by TGF-β.

Keywords: FGF8; TGF-β; Androgen; Oligonuceotide microarray

Transforming growth factor (TGF)-β is a multifunctional peptide growth factor involving various physiological and pathological cellular responses. In general, TGF-β serves as an inhibitor of cell growth [1]. The TGF-β signals are transduced into the nucleus through Smad proteins, resulting in the transcriptional activation of growth-inhibitory genes. For instance, $p15^{INK4B}$, one of the cyclin-dependent kinase inhibitors (CDKIs), is activated in response to TGF-β in cancer cells, leading to growth arrest [2,3]. In contrast, recent reports have shown that TGF-β is also involved in cancer progression mainly through the epithelial–mesenchymal transition (EMT) [4], known as a phenomenon in which cancer cells acquire more aggressive and invasive phenotypes than before by loosing epithelial gene expressions and gaining mesenchymal ones. In addition, TGF-β facilitates the expressions of extracellular matrix proteins and matrix remodeling proteins [5], also supporting the cancer invasion. Thus, the functions of TGF-β seem to be considerably varied among cancer cells.

An androgen-dependent mouse mammary carcinoma SC-3 cell line is one of the best in vitro models for understanding the growth mechanism of human hormone-responsive cancers. Our earlier reports have clearly demonstrated that *fgf8* plays an essential role in the androgen-dependent growth of SC-3 cells [7], and that FGF8 is involved in the growth of human prostate and breast cancers [8–10]. In our previous report, it was also demonstrated that TGF-β suppresses the androgen-dependent growth of SC-3 cells [11], indicating that SC-3 cells preserve the TGF-β signaling. Recently, it has been reported that the transcription of an androgen-regulated prostate-specific antigen (PSA) gene is repressed by the overexpression of *Smad3* [6], suggesting that TGF-β signals are involved in the transcriptional control of androgen-regulated genes in a repressive manner. This finding prompted us to investigate TGF-β-responsive genes in SC-3 cells using an oligonucleotide microarray method. In this analysis, *fgf8* was

* Corresponding author. Tel.: +81 285 58 7330; fax: +81 285 44 8467.
E-mail address: atanaka@jichi.ac.jp (A. Tanaka).

0960-0760/$ – see front matter © 2005 Elsevier Ltd. All rights reserved.
doi:10.1016/j.jsbmb.2005.01.031

by far the most markedly regulated gene in response to TGF-β. We further investigated the roles of the transcriptional repression of *fgf8* in TGF-β-mediated growth arrest in SC-3 cells.

1. Materials and methods

1.1. Cells

The SC-3 cells used in this study were established from an SC115 tumor. The method for cloning and the culture conditions were described previously [7]. For the establishment of stably FGF8-expressing SC-3 cells, pKANTEX93-FGF8 plasmid, kindly gifted from Dr. Shitara at Kyowa Hakko Kogyo, was transfected into SC-3 cells, and stably FGF8-expressing SC-3 cells were isolated.

1.2. Cell growth

The method for the MTT assay was described previously [9]. Briefly, SC-3 cells were plated onto a 96-well plate (3×10^3 per well) in a serum-free basal medium (DMEM:Ham's F-12 (1:1, v/v)), supplemented with 2% fetal bovine serum (FBS) treated with dextran-coated charcoal (dcc). The next day, the cells were stimulated with 50 ng/ml recombinant mouse FGF8 (R&D Systems, Minneapolis, MN, USA) in the presence or absence of various concentrations of recombinant human TGF-β1 (R&D Systems) under the serum-free condition. After 72 h of further incubation, MTT was added to the medium at a final concentration of 1 mg/ml. After another 4-h incubation, formazan substrates were collected, resolved with DMSO, and then measured at an absorbance of 570 nm, with reference at 690 nm.

1.3. RNAs

SC-3 cells were plated onto 100 mm-dishes (1.0×10^6 cells/dish) in a basal medium supplemented with 2% dcc-treated FBS under an androgen-free condition. The next day, the cells were stimulated with 10 nM testosterone in the presence or absence of 10 ng/ml TGF-β1 under the serum-free condition. Total cellular RNAs were prepared by an acid guanidium isothiocyanate–phenol–chloroform method at 12 h for the oligonucleotide microarray analysis. For the real-time PCR, total cellular RNAs were prepared using an RNeasy Kit (Qiagen GmbH, Hilden, Germany) at 0, 6, 12 and 24 h. Poly (A) RNAs were purified using the Oligotex-dT30 mRNA Purification Kit (TAKARA Biochemicals, Kyoto, Japan).

1.4. Oligonucleotide microarray analysis

The oligonucleotide microarray analysis was performed using a murine genome GeneChip U74A array (Affymetrix, Santa Clara, CA, USA) according to the standard protocols supplied by Affymetrix. Briefly, double-stranded cDNAs were synthesized from 1 μg of poly (A) RNA using the Superscript Choice System (Invirtogen, Carlsbad, CA, USA), then biotin-labeled cRNAs were prepared from these synthesized cDNAs by an RNA Transcript Labeling Kit (Enzo Life Sciences, Farmingdale, NY, USA). The fragmented cRNAs were hybridized with the U74A array for 16 h at 45 °C and 60 rpm. The array was washed on a GeneChip Fluidics Station 400 (Affymetrix) using an automated program, and the signals were then detected by a GMS 418 array scanner (Affymetrix). Scanned outputs were analyzed by Affymetrix software. Although the background levels were below 100, genes showing values lower than 200, either after the induction of TGF-β-inducible genes or before the repression of TGF-β repressive genes, were excluded because of their marginal expression.

1.5. Real-time PCR

Single-stranded cDNAs were synthesized using Superscript III (Invitrogen) according to the manufacturer's instructions from 1 μg of total cellular RNAs using an oligo dT primer. The PCR products were monitored by an ABI PRISM 7700 (Applied Biosystems, Foster City, CA, USA) using TaqMan probes. Primer sets used here were: mouse *fgf8*, 5′-CTGCTGTTGCACTTGCTGGT-3′ (forward primer); 5′-TCCCTCACATGCTGTGTAAAATTAG-3′ (reverse primer); Fam-CTCTGCCTCCAAGCCCAGGTAACTGTT-Tamra (TaqMan probe); mouse prostate stem cell antigen (PSCA), 5′-GGCTGAGATGGGATGGACTG-3′ (forward primer); 5′-CTGGGACTCCTGGTGCCTC-3′ (reverse primer); Fam-CAGAAATGGAGCTGGGAGGTGGGTG-Tamura (TaqMan probe); mouse lipocalin 7, 5′-GGAGGA-CAGTCGCGTACACA-3′ (forward primer); 5′-TGCCTCC-TGGAGTAGCCCTT-3′ (reverse primer); Fam-TGTCCTT-AAGCCGTTCCCTCGGAGC-Tamra (TaqMan probe); mouse β-actin, 5′-AGTGTGACGTTGACATCCGTAAAG-3′ (forward primer); 5′-AATGCCTGGGTACATGGTGGTA-3′ (reverse primer); and Fam-CCTCTATGCCAACAC-AGTGTTGTCTGGTG-Tamra (TaqMan probe).

1.6. Detection of apoptosis

The caspase 3 activity was measured using a Caspase 3 Assay Kit (Sigma–Aldrich, St. Louis, MO, USA). Briefly, SC-3 cells (2.5×10^6 cells/dish) were plated and stimulated with 10 nM testosterone in the presence or absence of 10 ng/ml TGF-β1 or 5 ng/ml recombinant mouse tumor necrosis factor (TNF)-α (PeproTech Inc., Rocky Hill, NJ, USA) for the indicated hours under a serum-free condition. The cell lysates were collected and suspended in the lysis buffer from the kit. After removal of the cell debris by centrifuguration, the peptide substrate acetyl-Asp-Glu-val-Asp-*p*-nitroanilide (Ac-DEVD-pNA) was added to the aliquots. After incubation for 2 h at 37 °C, the samples were measured at an absorbance of 405 nm.

Apoptosis was also evaluated by the TUNEL method using an ApopTag Peroxidase In Situ Apoptosis Detection Kit (CHEMICON Interntional, Temecula, CA, USA). Briefly, SC-3 cells were plated onto 4-well-chamber slides, and then the cells were treated with test compounds for the indicated hours. After fixation with 1% paraformaldehyde (pH 7.4) for several hours at 4 °C, the slides were washed and the nucleotide nick ends were tailed with digoxigenin-dNTPs using terminal deoxynucleotidyl transferase (TdT) for 1 h at 37 °C. The slides were then incubated with an anti-digoxigenin antibody conjugated to peroxidase, and immunostained with 3,3′-diaminobenzidine tetrahydrochloride. Positive cells per one hundred cells were counted in four different areas on each slide.

Table 1
Top 40 of TGF-β-inducible genes in androgen-stimulated SC-3 cells

No.	Genbank accession	Gene symbol	Gene name	Microarray data		
				T[a]	+TGF-β[b]	Ratio
1	X91617	Xrn1	5′–3′ Exoribonuclease 1	4.9	258.4	52.7
2	AW125043	C820004H04Rik	RIKEN cDNA C820004H04 gene	15.4	588	38.2
3	X05546	Ccrn4l	CCR4 carbon catabolite repression 4-like (*S. cerevisiae*)	367.3	13059	35.6
4	M58564	Zfp36l2	Zfp36l2: zinc finger protein 36, C3H type-like 2	8.7	274.1	31.5
5	Y17793	Robo1	Roundabout homolog 1 (*Drosophila*)	7.6	204.2	26.9
6	AA797843	D11Ertd530e	DNA segment, Chr 11, ERATO Doi 530, expressed	11.8	269.1	22.8
7	AB010383	Ror1	Receptor tyrosine kinase-like orphan receptor 1	16.1	359.3	22.3
8	AW060401	Arhq	ras homolog gene family, member Q	96.2	1957.8	20.4
9	X07888		*M. musculus* HMGCR gene for 3-hydroxy-3-methylglutaryl coenzyme A reductase, exon 2	18.4	360.3	19.6
10	AF002823	Bub1	Budding uninhibited by benzimidazoles 1 homolog (*S. cerevisiae*)	12.4	235.9	19.0
11	AW228840		up22f10.×1 NCI_CGAP_Mam2 Mus musculus cDNA clone, IMAGE:2655115 3′, MRNA sequence	15.6	285.5	18.3
12	AW046027	2010204I15Rik	RIKEN cDNA 2010204I15 gene	13.2	220.9	16.7
13	X57349	Trfr	transferrin receptor	16.9	280.5	16.6
14	AF076845	Hus1	Hus1 homolog (*S. pombe*)	22.7	369.2	16.3
15	AV003873	Clu	Clusterin	15.9	257.3	16.2
16	AW045443	Mef2a	Myocyte enhancer factor 2A	44.3	702.4	15.9
17	X53250	Zfa	Zinc finger protein, autosomal	15.9	251.1	15.8
18	D50032	Tgoln2	*trans*-Golgi network protein 2	16.2	253.9	15.7
19	AB035174	Siat7f	Sialytransferase 7 ((alpha-*N*-acetylneuraminyl 2,3-betagalactosyl-1,3)-*N*-acetyl galactosaminide alpha -2,6-sialytransferase) F	15.6	234.4	15.0
20	AF100777	Wisp1	WNT1-inducible signaling pathway protein 1	72.3	1080.2	14.9
21	M60474	Marcks	Myristoylated alanine rich protein kinase C substrate	59.7	873.4	14.6
22	AI848924	Parg	Poly (ADP-ribose) glycohydrolase	29.2	418.7	14.3
23	D86603	Bach1	BTB and CNC homology 1	15.8	220.4	13.9
24	D12713		Mus musculus gene for MSEC66, complete cds	25.1	326.8	13.0
25	D26532	Runx1	Runt related transcription factor 1	62.9	788	12.5
26	AV138783	Gadd45b	Growth arrest and DNA-damage-inducible 45 beta	62.7	779.3	12.4
27	AF084480	Baz1b	Bromodomain adjacent to zinc finger domain, 1B	20.2	242.8	12.0
28	U68182	Gcnt2	Glucosaminyltransferase, I-branching enzyme	40.8	440.4	10.8
29	AI642553	Iqgap1	IQ motif containing GTPase activating protein 1	47.7	503.8	10.6
30	AI839116	2310034L04Rik	RIKEN cDNA 2310034L04 gene	47.3	497.8	10.5
31	X57349	Trfr	Transferrin receptor	54	557.1	10.3
32	AV380793	Eif4g1	Eukaryotic translation initiation factor 4, gamma 1	97.3	964.4	9.9
33	AF000294	Pparbp	Peroxisome proliferator activated receptor binding protein	40.7	399.8	9.8
34	AW214136		uo40c11.×1 NCI_CGAP_Lu29 Mus musculus cDNA clone IMAGE:2645012 3′ Similar to TR: O89815 O89815 POL POLYPROTEIN, MRNA sequence	142.8	1362.2	9.5
35	AJ238636	Entpd5	Ectonucleoside triphosphate diphosphohydrolase 5	22.4	210.1	9.4
36	AA763004		Mus musculus cDNA clone IMAGE:6331951, partial cds	147.1	1373.2	9.3
37	X57349	Trfr	Transferrin receptor	46.2	425.3	9.2
38	U14135	Itgav	Integrin alpha V	27.2	249.1	9.2
39	U73478	Anp32a	Acidic (leucine-rich) nuclear phosphoprotein 32 family, member A	239.9	2167.7	9.0
40	D87900	Arf3	ADP-ribosylation factor 3	45	406.3	9.0

[a] T, 10 nM testosterone
[b] +TGF-β, 10 nM testosterone plus 10 ng/ml of recombinant human TGF-β1.